HIGHWAY RESEARCH RECORD

Number 342

Environmental Effects on Concrete

5 Reports

Subject Area

32 Cement and Concrete

HIGHWAY RESEARCH BOARD

DIVISION OF ENGINEERING NATIONAL RESEARCH COUNCIL
NATIONAL ACADEMY OF SCIENCES—NATIONAL ACADEMY OF ENGINEERING

WASHINGTON, D.C. 1970

ISBN 0-309-01847-1

Price: $2.00

Available from

Highway Research Board
National Academy of Sciences
2101 Constitution Avenue
Washington, D.C. 20418

Department of Materials and Construction

R. L. Peyton, Chairman
State Highway Commission of Kansas, Topeka

R. E. Bollen and W. G. Gunderman
Highway Research Board Staff

CONCRETE DIVISION

Bryant Mather, Chairman
U. S. Army Engineer Waterways Experiment Station
Jackson, Mississippi

COMMITTEE ON PERFORMANCE OF CONCRETE—PHYSICAL ASPECTS

(As of December 31, 1969)

Thomas D. Larson, Chairman
Pennsylvania State University, University Park

Philip D. Cady, Secretary
Pennsylvania State University, University Park

Howard T. Arni
James E. Backstrom
Cecil H. Best
D. L. Bloem
R. H. Brink
William P. Chamberlin
Herbert K. Cook
Clarence DeYoung
Wade L. Gramling
Paul Klieger
William B. Ledbetter
F. E. Legg, Jr.
John Lemish
Bryant Mather
J. F. McLaughlin
Howard H. Newlon, Jr.
Melville E. Prior
F. A. Renninger
Hollis B. Rushing
V. R. Sturrup
Patrick H. Torrans
R. P. Vellines
Richard D. Walker
E. A. Whitehurst
George H. Zuehlke

Foreword

Predicting the durability and volume stability of concrete in natural environments depends ultimately on a knowledge of diurnal and seasonal changes in its moisture and temperature regime. Present technology, however, allows only a gross empirical estimate of these factors. While our understanding of the mechanisms by which moisture and temperature affect concrete performance has advanced significantly, our ability to characterize the moisture-temperature environment and to predict the concrete's response to it is sorely deficient.

The five papers that appear in this RECORD deal with various aspects of this problem. The first three of these are reviews and the last two report the results of specific research.

Cady reviews the limitations of available climatological data in defining the atmospheric component of the highway environment. He points out that local variations in climate within any given climatic domain may be large enough to seriously impair the usefulness of much traditional climatological data. He then introduces the concept of micro-climatology and concludes that our primary concern in the future must be to develop the technology for predicting the critical micro-environmental conditions that result in localized problems.

Harmathy reviews the prevalent theories of moisture transport in porous systems and discusses the more complex mechanism of simultaneous heat and moisture transport in concrete. The subject is basic to understanding how concrete and other highway materials respond to the moisture and temperature environment at their boundaries.

The problem of in-place measurement of moisture content for various highway components is reviewed by Monfore. Significantly, he reminds us that the physical properties of highway materials are influenced not only by the total amount of water that they contain but also by the physical state of the water as well. Thus, after reviewing the various approaches to moisture measurement, he warns that the selection of a method should be based on the material property that is of prime importance because different measurement methods are sensitive to water in different physical states. Monfore concludes that there is, at present, no single instrument satisfactory for measuring the water contents important to all aspects of highway materials behavior under all conditions.

Through a controlled field study of simulated pavement slabs, Stark attempted to determine the effect of subbase type on the accumulation of moisture and the development of D-cracking in pavement concrete. His conclusion after two years of observation—that moisture content increased gradually regardless of subbase type—supports accumulating evidence that, without artificial subbase drainage, the underside of pavement slabs will attain and retain a high level of moisture. Stark's paper, with the discussion by Cady and Carrier, provides information on the stacked-disc technique of monitoring moisture changes in pavement concrete that should be useful to other investigators in this field.

A new heat transfer model for studying temperature and temperature-related effects in a multilayered pavement system is presented by Dempsey and Thompson. The new model incorporates climatological data and the physical and thermal properties of the pavement layers. It provides an efficient new tool for research into environmental effects on highway pavement components.

—W. P. Chamberlin

Contents

Climatological Literature Pertaining to Performance of Highway Concrete

PHILIP D. CADY, Pennsylvania State University

Drawing from literature, the current state of knowledge regarding the effects of environmental factors on the serviceability of concrete pavements is explored. The basic parameters involved are those that comprise and define climatic domain. However, it is shown that wide variations of these parameters (e.g., temperature) can occur over relatively short distances within a given climatic domain because of topographic, geologic, hydrologic, and floral differences. Thus, while the problem is related to microclimate, the measurements and data currently available are, for the most part, representative of the macroscale. It is concluded that if the prediction of the occurrence of extremes in microenvironmental conditions that lead to localized deterioration of concrete pavement components is ever to be realized, it will first be necessary to determine the critical limits of the various environmental parameters, individually and in combination, and the development of the technology to predict accurately the occurrences of the critical conditions.

•THIS rather pertinent statement was made more than 40 years ago (1): "Any definite information, easily available to the engineer and contractor, about any climatic factor enables them to more surely build good roads." The occasion was a report of an HRB subcommittee charged with the task of preparing an outline of the information regarding the various phases of climate that affect the building, maintenance, and use of highways. This statement is certainly as applicable today as it was in 1929. Furthermore, it appears that, while our knowledge of the mechanisms by which environmental factors influence the performance of highway components has advanced significantly, our knowledge of the critical limits for these factors is still sorely lacking. Even more frustrating is our inability to predict, with any degree of certainty, where the environmental and material factors will combine to create a condition adversely affecting the serviceability of highway pavements.

MACROENVIRONMENT VERSUS MICROENVIRONMENT

One of the major reasons for this problem is the fact that climatological data are usually relied on to define the atmospheric part of the environment. Climatological data, of course, purport to represent conditions over relatively large areas. It can be shown, on the other hand, that environmental conditions can vary greatly over relatively short distances. For example, Geiger (2) reported that only one night with a temperature below freezing (29 F) was recorded during a particular month of May at the meteorological station in Munich, Germany. In the same month, 23 nights with below freezing temperatures as low as 6 F above zero were measured in the air layer near the ground only 12 miles outside the city. In addition to the relatively great distances between weather stations, the problem is further compounded by the fact that the weather instruments from which climatological data are compiled are located at a height of about 6 ft above the ground. Geiger presented additional data showing that

Paper sponsored by Committee on Performance of Concrete—Physical Aspects and presented at the 49th Annual Meeting.

the extremes of temperature and humidity are considerably more pronounced in the air layer at the ground surface than they are at the level of the meteorological instruments.

The major hurdle in the path of associating environmental factors with pavement performance now becomes eminently clear. It is one of scale—we are going to have to shift our attention from the macroenvironmental to the microenvironmental level.

In speaking of environment, micro or macro, as related to pavement structures, it must be recognized that we are dealing with two domains—the atmosphere and the earth. Furthermore, these two domains are not independent. For example, it can be shown that microclimate is strongly influenced by topography. It should be readily evident that the variations in environment associated with the earth will be great, perhaps greater than those associated with the atmosphere.

USE OF CLIMATOLOGICAL DATA

In view of the variability of microclimate over relatively small areas, it becomes clear that what we have here is a problem in sampling. This immediately implies the need for a statistical approach for both the gathering and the analysis of environmental data. Thom (3), for example, stated it this way: "For the large area of planning decisions for years, even many years in the future, the statistical analysis of historical data resulting in the climatological prediction is required." He goes on to state, "There is today a good body of valid climatological analysis available which can give unbiased climatological prediction for the development of engineering design data almost anywhere in the world." This statement appears to be overly optimistic in view of the high degree of variability in the microclimate within a given climatic domain, as illustrated earlier. The engineering design data and climatological data are related by a so-called "weather design value," which Thom defines as, "The magnitude of a meteorological variable which, when used in the design of an engineering system, nonmeteorological factors having been accounted for jointly or independently, will assure with a given probability that the system will adequately meet a set of prescribed design requirements."

We might ask ourselves at this point, to what extent have environmental data been correlated with design of pavement structures to date? Examples of compilation and use of climatological data are worth mentioning. Eno's 1929 report (1) contains a wealth of information gleaned from publications of the U.S. Weather Bureau. It includes annual variation of temperature at various locations in the United States, lowest temperatures ever observed (through 1922) throughout the United States, lowest monthly mean temperatures throughout the United States for the months of April and November, average lowest temperatures throughout the United States, number of times in a 20-year period that the lowest temperature was 9 F or more below the average lowest temperature throughout the United States, average date when the mean daily temperature falls below 35 F throughout the United States, average dates of last killing frost in the spring throughout the United States, average dates of first killing frost in the fall throughout the United States, average percentage of sunshine in summer throughout the United States, annual average wind velocity throughout the United States, average minimum relative humidity (October) throughout the United States, evaporation rates during warm season throughout the United States, percentage of annual rainfall that occurs each month for various regions of the United States, average annual precipitation throughout the United States, total number of periods of 20 consecutive days or more without 0.25 in. of precipitation in 24 hours throughout the United States, average annual snowfall throughout the United States, average annual number of days with snow cover throughout the United States, and average annual number of clear days throughout the United States. This long list is mentioned to illustrate the varied types of climatological data that were available from the Weather Bureau in 1929 and, presumably, are still being gathered by that agency.

Siple (4) in 1952 presented climatic and geographic data to depict the distribution of frost heave elements and to predict the severity of frost heave.

In 1956, Jumikis (5) analyzed 55 years of U.S. Weather Bureau data in New Jersey and found a strong periodicity of occurrence of severe winters. He also noted that the first damage to roads occurs when the freezing index value of 285 degree-days is reached in any given winter.

Russam and Coleman (6) in 1961 examined the climatic factors related to subgrade moisture conditions.

Larson and co-workers (7) in 1968 presented climatological information compiled from U.S. Weather Bureau data related to bridge deck durability in Pennsylvania. This included average number of freeze-thaw cycles, average annual precipitation, and ASTM weathering index.

The design manual (8) of the U.S. Army Corps of Engineers provides one of the best sources of information with regard to severity of winters at various locations. The manual provides plots of the "design freezing index" covering the areas of the globe where freezing conditions may be encountered.

The examples of sources, compilation, and use of climatological data, just discussed, point up the large number of climatological parameters that have to be taken into account. This brings up another problem: How can the various parameters be combined to provide a unique descriptive factor that can be related to engineering design factors? The Corps of Engineers "design freezing index" and ASTM's "weathering index" are limited attempts to arrive at such a factor. Thornthwaite (9) in 1948 devised a system for rational classification of climate based on precipitation, evapotranspiration, and temperature that might prove to be of use to the highway engineer.

MICROENVIRONMENTAL STUDIES

So far we have dealt only with the gathering and use of climatological data. However, as mentioned earlier, the microclimate within any given climatic domain is so variable as to greatly impair the usefulness of climatological data. In recognition of this fact, numerous studies have been undertaken to evaluate the microenvironment under various specified conditions. Examples of several such studies will be cited briefly for illustrative purposes.

Crabb and Smith (10) in 1953 described a series of extensive experiments in which seasonal soil temperature variations were related to various types of ground cover.

In 1958, Guinnee (11) reported on field studies of subgrade moisture content carried out by the Missouri Department of Highways over a 5-year period. This study entailed considerably detailed measurement of temperature and moisture distributions in pavement subgrades as related to various design parameters.

In a 1968 study for the Pennsylvania Department of Highways, Fang (12) examined the influence of temperature and other climatic factors on the performance of soil pavement systems using data from specific test locations at the AASHO Road Test. Groundwater level fluctuations, frost penetration, and soil temperature distributions and variations were examined in terms of the air temperatures, season, ground cover, pavement type, and amount of traffic for the specific test locations.

Emerson (13) in 1968 reported on an extensive study on bridge temperatures relative to air temperatures.

In 1969, Straub and co-workers (14) described a test installation in which the temperature and moisture distributions were examined beneath pavement and shoulders as a function of the color of shoulders.

In one of two known very recent studies, Larson and co-workers (15) carried out limited tests for the Pennsylvania Department of Highways to evaluate the moisture distribution in a concrete pavement as a function of precipitation, season, topography, and geology of the test area. This group is currently carrying out similar studies on two concrete bridge decks. Moisture distribution studies in concrete slabs on grade were also recently carried out by Stark (16).

CONCLUSIONS

Although the examples just related indicate that work is progressing in an effort to relate microenvironmental factors to those conditions known to be detrimental to

pavement structures, it is evident that much remains to be done. The current state of the art in environmental effects on highway components, then, can be summarized as follows: Considerable data are available on the climatic parameters and the mechanisms by which environmental factors adversely affect highway components. However, there are distinct shortcomings in our ability to predict the occurrence of extremes in microenvironmental conditions that lead to localized problems. The determination of the critical limits of the various environmental parameters, individually and in combination with each other, and the development of the technology to predict accurately the occurrences of critical conditions must be our primary concern in the future.

ACKNOWLEDGMENT

I would like to take this opportunity to thank Ed Bellock, one of my students, for his assistance in researching this paper.

REFERENCES

1. Eno, F. H. The Influence of Climate on the Building, Maintenance, and Use of Roads in the United States. HRB Proc., Vol. 9, 1929, pp. 221-249.
2. Geiger, Rudolf. The Climate Near the Ground. 2nd ed., Harvard Univ. Press, 1966, 611 pp.
3. Thom, H. C. S. Application of Climatological Analysis to Engineering Design Data. Draft of a paper to be published in Revue Belge de Statistique et de Recherche Opérationelle, 1969, 17 pp.
4. Siple, P. A. Climatic Aspects of Frost Heave and Related Ground Frost Phenomena. HRB Spec. Rept. 2, 1952, pp. 10-16.
5. Jumikis, A. R. Cold Quantities in New Jersey, 1901-1955. HRB Bull. 135, 1956, pp. 119-123.
6. Russam, K., and Coleman, J. D. The Effect of Climatic Factors on Subgrade Moisture Conditions. Geotechnique, Vol. 11, No. 1, March 1961, pp. 22-28.
7. Larson, T. D., Cady, P. D., and Price, J. T. Review of a Three-Year Bridge Deck Study in Pennsylvania. Highway Research Record 226, 1968, pp. 11-25.
8. U.S. Army Engineer School. Student Reference, Section I, Soils Engineering. Vol. 2, Chaps. 6-9, S.002, 1967.
9. Thornthwaite, C. W. An Approach Toward a Rational Classification of Climate. The Geographical Review, Vol. 38, No. 1, 1948, pp. 55-94.
10. Crabb, G. A., Jr., and Smith, J. L. Soil-Temperature Comparisons Under Varying Covers. HRB Bull. 71, 1953, pp. 32-80.
11. Guinnee, J. W. Field Studies on Subgrade Moisture Conditions. HRB Spec. Rept. 40, 1958, pp. 253-267.
12. Fang, H. Y. Influence of Temperature and Other Climatic Factors on the Performance of Soil-Pavement Systems. Fritz Eng. Lab. Report No. 350.1, Lehigh Univ., Aug. 1968, 39 pp.
13. Emerson, Mary. Bridge Temperatures and Movements in the British Isles. RRL Rept. LR 228, 1968, 25 pp.
14. Straub, A. L., Dudden, P. E., and Moorhead, F. T. Frost Penetration and Moisture Changes Related to Highway Pavement Shoulder Color. Highway Research Record 276, 1969, pp. 39-49.
15. Larson, T. D., Cady, P. D., Browne, F. P., Carrier, R. E., and Lowry, L. L. Moisture Distribution in a Pavement Slab. In Methods for Analysis of Hardened Concrete, Penn. State Univ. Materials Research Rept., Sept. 1969, pp. 202-217.
16. Stark, David. Field and Laboratory Studies of the Effect of Subbase Type on the Development of D-Cracking. Paper presented at the 49th Annual Meeting and published in this Record.

Moisture and Heat Transport With Particular Reference to Concrete

T. Z. HARMATHY, Division of Building Research,
National Research Council of Canada

Over the years three theories have gained general acceptance in explaining the movement of moisture in porous media: the diffusion theory, the capillary flow theory, and the evaporation-condensation theory. Because a wet porous solid actually consists of at least three phases, the mechanism of simultaneous moisture and heat transport is very complex. During the capillary and funicular states of the system, moisture moves primarily by a convective transport mechanism, and the rate of moisture movement is relatively insensitive to the properties of the solid matrix. In the pendular state, the evaporation-condensation mechanism is predominant, and the rate of moisture migration depends on the complexity of the pore structure. For fresh concretes the related problems are augmented by the hydration reactions.

•FOR several decades soil scientists and chemical engineers have shown considerable interest in the problem of moisture migration in porous media. Soil scientists have been primarily concerned with the movement of moisture at relatively high pore saturations and have developed rather complex mathematical models to describe the process under both isothermal and non-isothermal conditions. Chemical engineers, being mainly interested in industrial drying operations, have paid considerably more attention to the effect of certain characteristics of the surroundings on the variation of total moisture content within the boundaries of the drying solid than to the internal mechanism of moisture migration.

DIFFUSION AND CAPILLARY FLOW THEORIES

Over the years several explanations have been offered for the migration of moisture in porous media. Three deserve detailed discussion: the diffusion theory, the capillary flow theory, and the evaporation-condensation theory. Symbols used in the equations that follow are defined at the end of the paper.

The movement of moisture by diffusion was proposed as the principal flow mechanism by Lewis (1), Tuttle (2), Sherwood (3), Newman (4), Childs (5), Kamei (6), and many others. The diffusion theory is based on the assumption that the moisture flux is proportional to the gradient of moisture concentration. For one-dimensional moisture flow

$$n = -\rho_m \chi \frac{\partial m}{\partial x} \tag{1}$$

where χ is assumed to depend only on some characteristics of the porous medium.

By combining Eq. 1 with the equation of continuity (7)

$$\rho_m \frac{\partial m}{\partial t} + \frac{\partial n}{\partial x} = 0 \tag{2}$$

Paper sponsored by Committee on Performance of Concrete—Physical Aspects and presented at the 49th Annual Meeting.

Fick's second law is obtained

$$\frac{\partial m}{\partial t} = \chi \frac{\partial^2 m}{\partial x^2} \tag{3}$$

which is formally identical to Fourier's law of heat conduction.

The inadequacy of the diffusion theory in describing the migration of moisture was pointed out by McCready and McCabe (8) and discussed in detail by Hougen and coworkers (9). Although a group of research workers attempted to achieve better agreement between theoretical and experimental data by regarding the diffusion coefficient, χ, as a function of moisture concentration, m, rather than constant, the search continued for the development of more accurate theories.

The fundamentals of the capillary flow theory were laid down by Buckingham (10) in 1907. Since that time the theory has undergone considerable change, initiated by Gardiner (11), Israelson (12), Edlefsen and Anderson (13), and others. In its latest version it is based on the assumption that the following relation exists between moisture flux and the gradient of the "total moisture potential," Φ,

$$n = -\rho_m K \frac{\partial \Phi}{\partial x} \tag{4}$$

where K, capillary conductivity, is not a constant but a function of moisture concentration.

Equation 4 is often referred to as Darcy's equation for unsaturated capillary flow. In it, as Edlefsen and Anderson (13) pointed out, the total moisture potential is identical to the partial specific Gibbs free energy (chemical potential) of the moisture in the porous medium, and can be expressed as

$$\Phi = gz + \Psi \tag{5}$$

where Ψ, the capillary potential, is also a function of the moisture concentration. In problems connected with soil moisture, the level of the water table is taken as the z = 0 level.

By combining Eqs. 4 and 5 with the equation of continuity, Eq. 2, the following equation is obtained for horizontal flow:

$$\frac{\partial m}{\partial t} = \frac{\partial}{\partial x} \left(\varkappa \frac{\partial m}{\partial x} \right) \tag{6}$$

where $\varkappa$, the coefficient of capillary diffusion, is defined as

$$\varkappa = K \frac{\partial \Psi}{\partial m} \tag{7}$$

Equation 6 can be recognized as a modified form of Fick's second law of diffusion with a diffusion coefficient dependent on moisture concentration.

Before solving Eq. 6, the $K = K(m)$ and $\Psi = \Psi(m)$ functions must be determined experimentally for the porous medium of interest. The nature of these functions has been studied by Richards (14), Philip (15), Schofield (16), and many others.

The capillary flow theory was further modified by Philip (17, 18, 19), Philip and de Vries (20), and de Vries (21) to include movement of water in the gaseous phase (in the pores of the solid), in the "adsorbed" phase, and under the effect of temperature gradient. These workers also added a second equation to the basic equation of capillary flow (Eq. 6 for horizontal flow) in order to balance the energy changes brought about by the movement and evaporation of moisture. Krischer in Germany (22, 23) and Lykov's school in Russia (24, 25), based on somewhat different reasonings, developed sets of equations closely resembling those of Philip and de Vries.

Chemical engineers applied the capillary flow theory in a different way. Based on the fundamental work of Haines (26), Ceaglske and Hougen (27), Pearse and co-workers (28), and Corben and Newitt (29) derived an expression for the moisture flux by balancing the capillary and gravitational forces, acting on a thread of water in the pores, against the frictional forces.

Before discussing the evaporation-condensation theory, it is desirable to examine briefly some common characteristics of wet porous solids and to discuss experimental findings concerning an important moisture and heat transport process—namely, drying.

THE POROUS SYSTEM

Difficulties in understanding the mechanism of moisture movement in porous solids were probably the result of inaccurate modeling of the system in which the moisture movement takes place. Many research workers assumed directly or implied by the use of certain laws (e.g., Eq. 1 for diffusion) that a porous solid is a single-phase system. In reality, a wet solid consists of at least three phases: (a) a solid phase, i.e., the material of the porous matrix; (b) a liquid (or absorbed) phase, which is essentially water; and (c) a gaseous phase, a mixture of air and water vapor. (Air can be regarded as a single component of the system.) The latter two are contained within the visible boundaries of the first. This three-phase system will be referred to hereafter as porous system for brevity.

In most practical problems it is permissible to regard the solid phase as a single-component, rigid material containing a network of interconnected pores and exhibiting, in macroscopic dimensions, isotropic characteristics.

The water in the liquid phase of the porous system is, to some extent, different from ordinary liquid water. In a few layers adjoining the pore surface, the water molecules are tightly held by a force field. These adsorbed molecules have very limited mobility and can move only by molecular transport processes, in other words, past each other on a molecular scale.

Outside the adsorbed layers the liquid water behaves more like water in narrow capillary tubes. This portion of the liquid phase, commonly referred to as capillary water, has a high degree of mobility. For this water, convection is the primary transport mechanism; that is, the molecules can move relatively freely in larger masses on a macroscopic scale.

In the gaseous phase, air and water molecules can move past each other by some molecular transport mechanism, mainly diffusion. In addition, the air and water molecules also move together in large masses, usually under the effect of pressure gradients.

It becomes obvious that because of the complexity of the system the diffusion theory cannot describe correctly the total moisture migration.

EQUILIBRIUM SORPTION RELATION

The water vapor concentration in the gaseous phase is generally not far removed from a value corresponding to the equilibrium sorption relation, which is an experimentally developed relation between the amount of liquid phase moisture, m (sometimes expressed in terms of relative saturation, m/ϵ), and the equilibrium vapor pressure, P_v (usually expressed in terms of the relative humidity in an equilibrium environment, P_v/P_v°). (In equilibrium, the partial pressure of water vapor, P_v, is the same in the environment as in the porous system.) The sorption relation depends on certain characteristics of the porous system. Three factors are of major importance: (a) the porosity of the solid matrix, ϵ, which determines the maximum amount of moisture that the solid can hold; (b) the specific surface, s (i.e., the magnitude of the internal pore surfaces per unit volume of the matrix), which determines the maximum amount of moisture that the solid can hold by adsorption; and (c) a constant, C, in the Brunauer-Emmett-Teller equation (30), which characterizes the affinity between the pore surfaces and the water molecules.

The sorption relation is normally obtained by experiment, although if ϵ, s, and C are known it is possible to obtain at least a rough estimate of it (31).

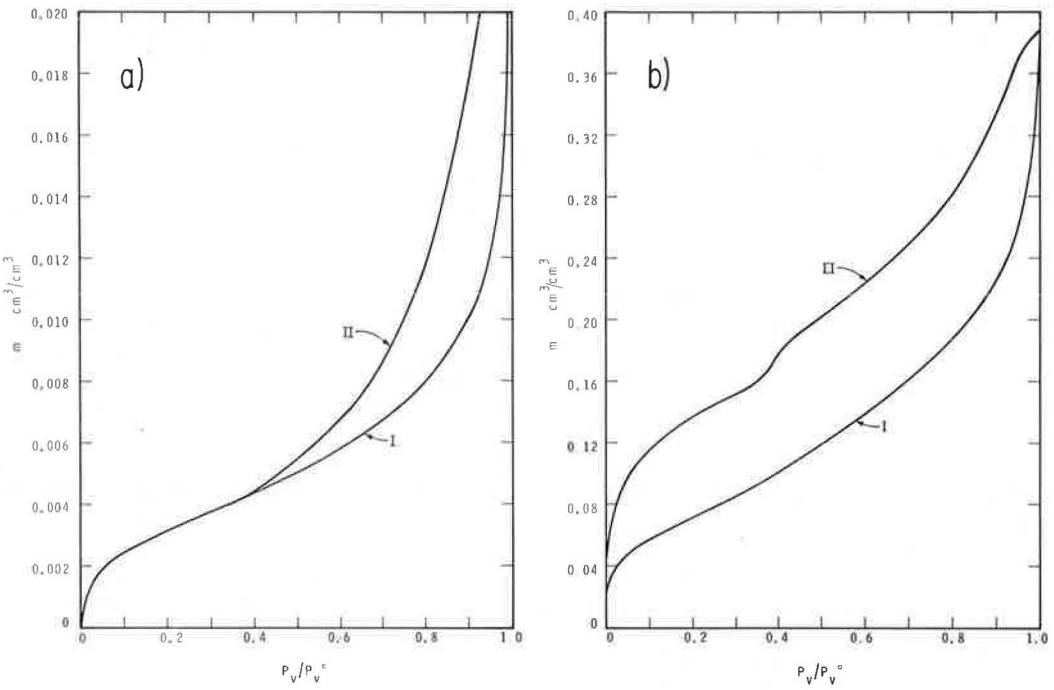

Figure 1. Sorption equilibria: (a) clay brick, (b) hydrated cement paste; curve I, adsorption; curve II, desorption.

Figure 1 shows the sorption relations for two building materials, a clay brick and a hydrated cement paste. The sorption relation for both materials is characterized by two curves, an adsorption curve obtained by a monotonic increase of the vapor pressure of the ambient air from 0 to P_v° through very small equilibrium steps, and a desorption curve obtained by the reverse procedure. (These curves are, to some degree, also dependent on the temperature, and therefore have to be obtained while keeping the temperature constant. For this reason they are often referred to as sorption isotherms.) Any point within the hysteresis loop formed by the two curves may represent an equilibrium condition for the system. The uncertainty concerning the effective equilibrium sorption relation presents difficulties in the rigorous treatment of moisture migration problems.

The sorption relation for clay brick (Fig. 1a) is a type commonly met among inorganic solids. The sorption hysteresis in the $0.4 < P_v/P_v^\circ < 1$ interval is caused by capillary water. The geometry of the surfaces of capillary water, determined by moisture concentration, controls (but not uniquely) the equilibrium vapor pressure in the pores by virtue of the Kelvin equation (32). In the $0 < P_v/P_v^\circ < 0.4$ interval the water molecules are held mainly by adsorption on the pore surfaces, and the sorption relation is uniquely determined by the specific surface, s, and the constant, C.

For hydrated cement paste (Fig. 1b) the hysteresis loop extends over the entire $0 < P_v/P_v^\circ < 1$ domain. The hysteresis in the $0 < P_v/P_v^\circ < 0.4$ interval is attributed to certain irreversible phenomena of a non-adsorptive nature (33). By comparing Figure 1a and 1b it may be seen that cement paste holds a much larger amount of moisture in equilibrium with any environment than does clay brick. For this reason it is usual to refer to cement paste and similar materials as hygroscopic materials.

If the porosity and specific surface of the porous matrix are known, it is possible, using the Kozeny equation (34), to make a rough estimate of the permeability of the matrix, which also plays some part in the process of moisture migration (as mentioned later).

DRYING

Drying is probably the most common process in which simultaneous moisture and heat transport play a dominant role. To gain insight into some practical aspect of moisture migration it seems desirable to review briefly the present state of knowledge concerning drying. For simplicity, the drying of a slab is discussed in an environment of constant temperature and relative humidity.

If the relative pore saturation is initially high, the average moisture content of the slab will decrease fairly fast during the first period of drying (Fig. 2a). This period is usually referred to as the constant rate period. Drying proceeds at an approximately constant rate roughly equal to the rate of evaporation from a free-water surface under identical environmental conditions. The temperature of the slab also is approximately constant (Fig. 2a) and, provided drying takes place in a fast airstream, is equal to the wet bulb temperature of the ambient air.

The first three curves in Figure 2b show the moisture distribution in the slab during the constant rate period. The relatively small gradients of moisture concentration clearly indicate that at this stage convection (capillary flow) is the principal mechanism of migration. From the previously mentioned finding concerning rate of drying, it is obvious that the evaporation of moisture takes place almost entirely at the surfaces of the slab.

Convective movement of moisture (i.e., the capillary flow mechanism) is limited to conditions of the porous system in which continuous water threads exist in the pores, namely, to the capillary and funicular states of the system (26, 27). As the amount of moisture in the pores decreases, the water threads gradually break up and a so-called pendular state is reached. The central cores of the pore channels are now occupied by the gaseous phase, and a still small but steadily increasing portion of the liquid phase moisture is held by adsorption on the pore surfaces. In this state the liquid moisture has a much lower degree of mobility, so that an increasingly larger fraction of the moisture migration takes place in the gaseous phase, partly by molecular transport phenomena (mainly diffusion) and partly by convection induced by pressure gradients.

This transport of moisture in the gaseous phase is possible only if the liquid moisture is first vaporized. Because some of the vaporized water often recondenses in some other zone of the porous system, it is usual to refer to this rather complex

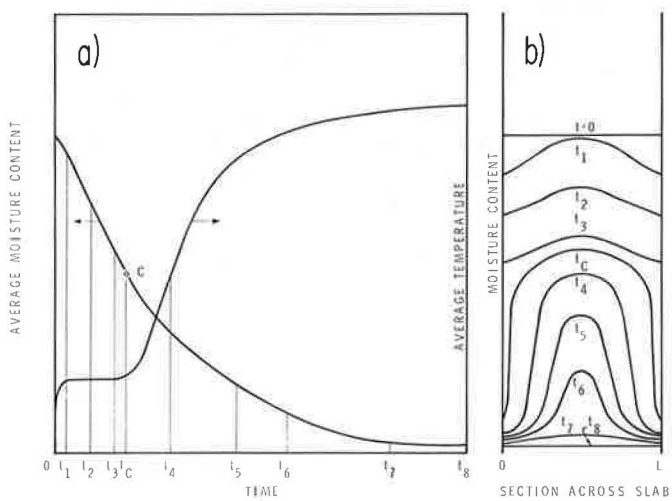

Figure 2. Characteristic curves of a drying porous slab: (a) average moisture content and temperature, (b) moisture distribution.

moisture transport mechanism as the evaporation-condensation mechanism. In it the equilibrium sorption relation, which controls the concentration of water molecules in the gaseous phase, plays an important part.

The constant rate period ends at the so-called "critical point" of drying, where the temperature of the slab takes a sharp upward trend. The moisture distribution at this point is an important characteristic of the pore structure (32).

After a brief transient period, during which the capillary flow mechanism still plays some role in moisture migration, the falling rate period sets in, characterized by the predominance of the evaporation-condensation mechanism. Figure 2a shows the generally steady decrease in the rate of temperature rise during this period, until finally the porous system attains equilibrium with its surroundings and all moisture and heat transport come to an end.

The curves in the lower part of Figure 2b shows various phases of the moisture distribution in the porous slab during the falling rate period. They indicate that the planes at which the bulk of moisture evaporation takes place gradually retreat from the surfaces toward the central plane of the slab, while the moisture concentration at the central plane remains high for a relatively long period.

Clearly, the larger the area of the internal pore surfaces in relation to pore volume, the larger is the portion of moisture retained at the onset of the pendular state and, in turn, the more significant is the evaporation-condensation mechanism in relation to the capillary flow mechanism. Because the rate of drying during the constant rate (or capillary moisture migration) period is relatively high and easily calculable, even without exact knowledge of the laws of capillary flow, the progress of drying during the falling rate period has long been the primary target for research and speculation among chemical engineers.

EVAPORATION-CONDENSATION THEORY

The evaporation-condensation theory has sprung from the desire to explain the movement of moisture in porous systems under the effect of temperature gradients. It was probably Bouyoucos (35) who first pointed out that in a closed system moisture moves opposite the temperature gradient. Many years later Vassilou and White (36) and Paxton and Hutcheon (37) demonstrated the importance of the equilibrium sorption relation in the moisture transport process. The dominant role of the evaporation-condensation mechanism when moisture moves under the effect of temperature gradient was further discussed by Gurr and co-workers (38), Hutcheon (39), and Kuzmak and Sereda (40).

By adopting simplifying assumptions concerning the porous system and the transport process, it is possible to describe mathematically the combined moisture and heat transport in porous media by the evaporation-condensation mechanism (32, 41). For the porous system the following assumption can be introduced: Although a porous system is in reality a three-phase system, the phases are so finely distributed that from a macroscopic standpoint it can be regarded as a quasi-one-phase system. This assumption implies, on the one hand, that it is possible to assign local values to the concentration of all components and all state variables of the system; and, on the other hand, that even though the system as a whole is generally a non-equilibrium system there is local equilibrium within each sufficiently small element of it. In this way the equilibrium sorption relation is automatically satisfied at each point of the system.

With respect to the transport process, the problem may be greatly simplified if it is assumed that the liquid phase is completely immobile; that is, that the water molecules must first be vaporized before they can move from one point to another in the system. As discussed earlier, for the pendular state of the system (or for the falling rate period of drying) this is a perfectly reasonable assumption.

With the aid of these assumptions and a few well-known principles, such as the laws of conservation of matter and energy, Darcy's law of convective mass transport through porous media (42), Fick's law of diffusion, and Fourier's law of heat conduction, a set of three basic equations will finally be obtained. For one-dimensional moisture and heat flow in a slab of thickness, L, these equations (41) are of the form

$$A_k \frac{\partial^2 \varphi}{\partial x^2} + B_k \frac{\partial^2 P}{\partial x^2} + C_k \frac{\partial^2 T}{\partial x^2} + D_k \left(\frac{\partial \varphi}{\partial x}\right)^2 + E_k \left(\frac{\partial P}{\partial x}\right)^2 + F_k \left(\frac{\partial T}{\partial x}\right)^2$$

$$+ G_k \frac{\partial \varphi}{\partial x} \frac{\partial P}{\partial x} + H_k \frac{\partial \varphi}{\partial x} \frac{\partial T}{\partial x} + J_k \frac{\partial P}{\partial x} \frac{\partial T}{\partial x} = K_k \frac{\partial \varphi}{\partial t} + L_k \frac{\partial P}{\partial t} + M_k \frac{\partial T}{\partial t} \quad (k = 1, 2, 3) \tag{8}$$

The most commonly applicable boundary conditions are as follows:

$$\left.\begin{aligned} \frac{\partial \varphi}{\partial x} &= (-1)^{\ell+1} \nu \alpha \left(\frac{RT}{PD}\right) (\varphi - \varphi_{\infty \ell}) \qquad (9) \\ \frac{\partial T}{\partial x} &= (-1)^{\ell+1} \frac{h}{k} (T - T_{\infty \ell}) \qquad (10) \\ P &= P_{\infty \ell} \qquad (11) \end{aligned}\right\} \quad \ell = 1 \text{ at } x + 0, \quad \ell = 2 \text{ at } x = L$$

When solved, these equations, together with the appropriate initial conditions

$$\varphi = \varphi(x, 0), \quad T = T(x, 0), \quad P = P(x, 0) \quad 0 \leq x \leq L \tag{12}$$

yield the complete moisture concentration, temperature, and pressure history of the wet porous slab in any transient process, provided that the system is in its pendular state.

For practical reasons, φ, the concentration of water vapor in the gaseous phase, has been selected as one of the three independent state variables of the system. This information is usually of no direct practical interest. It is used to calculate the moisture concentration history of the system by utilizing the equilibrium sorption relation, which is in fact a relation between m and φ ($=P_v/P$).

Some of the coefficients $A_1 \ldots M_3$ are equal to zero. Others are, in general, functions of (a) the three state variables, φ, P, and T, and (b) the following material characteristics: specific heat of all components, density of all components, thermal conductivity of all components, porosity and permeability of the solid matrix, coefficient of diffusion of water vapor in air, viscosity of gaseous phase, equilibrium sorption relation, and heat of sorption.

Figure 3 shows the computed moisture concentration, temperature and pressure history of a 1-cm thick brick slab in a drying process.

Equations 8 to 12 can be solved only with high-speed computers. It is possible, however, to draw a few conclusions concerning the rate of moisture movement in a porous system, either simply from some characteristics of the solid or from an exploratory drying test carried out on a thin slab cut from the solid.

SOME FACTORS AFFECTING THE RATE OF MOISTURE MIGRATION

During the capillary and funicular states of the porous system (i.e., at relatively high pore saturations), the rate of moisture movement is relatively insensitive to the properties of the system and depends mainly on external factors such as temperature and water vapor concentration of the ambient air and on air velocity, which affects the coefficients of heat and mass transfer at the surfaces.

These transfer coefficients continue to play some part in the moisture migration process, even during the pendular state (i.e., during the falling rate period of drying). Nevertheless, at this state the internal characteristics of the system become of primary importance. Because liquid moisture has to be vaporized to move from one location to another and because the heat of desorption is obtained by conduction from the surface of the system, it is clear that, other conditions being equal, moisture migration in a drying process is faster if the solid matrix is of a higher thermal conductivity.

One can also expect that the rate of moisture migration will be higher in solids of relatively simply pore structure. The simplicity of the pore structure is characterized

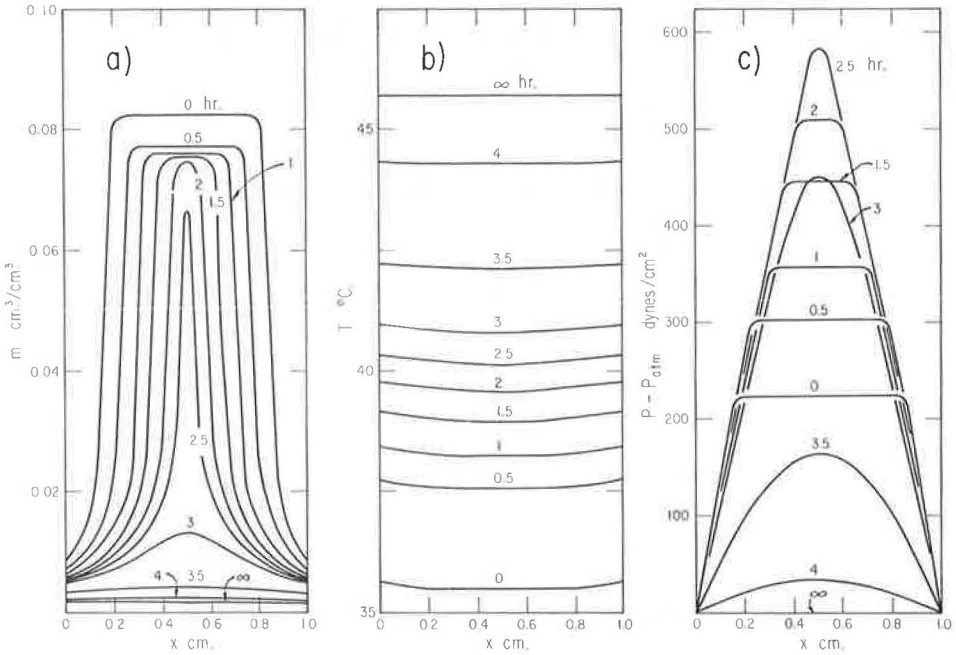

Figure 3. Computed distribution curves in simulation of a falling rate drying process (41).

by low values of the specific surface [by virtue of the previously mentioned Kozeny equation (32, 34) these also imply high permeabilities] and, in turn, by low equilibrium moisture concentrations, as reflected by the adsorption and desorption isotherms over the $0 < P_v/P_v^\circ < 0.9$ interval (Fig. 1a). Because such solids contain relatively small amounts of moisture at the critical point and retain very little residual moisture at the end of a drying process, one may presume that the moisture content at the critical point and the moisture retention of an exploratory slab specimen at the completion of the drying test are rough measures of the "resistance" of the solid matrix to moisture movement during the pendular state. (The residual moisture concentration is usually represented by a point within the hysteresis loop at a value of P_v/P_v° equal to the relative humidity of the environment.)

Figure 4 shows the results of drying tests performed under identical environmental conditions on five 1-cm thick slabs: a hydrated portland cement paste, two lightweight concretes, one autoclaved normal weight concrete, and a clay brick. The drying curves have been slightly displaced along the time axis in order to have the critical points line up at 0.5 hour. Information concerning the materials is given in Table 1.

Figure 4 shows clearly that the rate of drying during the constant rate period depends very little on the characteristics of the system. The figure also confirms the previously discussed principles concerning the rate of moisture movement during the falling rate period.

EFFECT OF MOISTURE CONTENT ON THERMAL CONDUCTIVITY

Very often, only the heat transport process is of practical interest in a process of simultaneous moisture and heat transport. It has always seemed very attractive, therefore, to reduce the complex problem of heat and moisture transport to a problem of heat conduction in a medium with a thermal conductivity dependent on the moisture concentration. In achieving this, many research workers have assumed that the thermal conductivity of the moist solid is always higher than that of the dry solid.

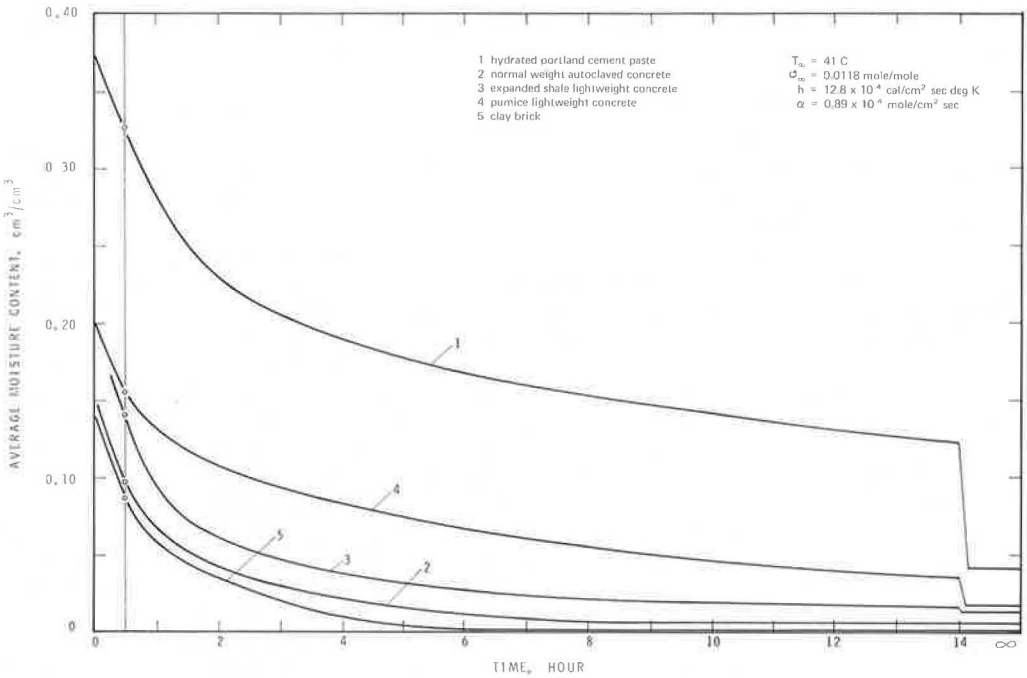

Figure 4. Drying experiments performed on 1-cm thick slabs.

TABLE 1

INFORMATION CONCERNING MATERIALS IN FIGURE 4

Material	Density (g/cm^3)	Thermal Conductivity (cal/cm sec deg K)	Porosity (cm^3/cm^3)	Specific Surface[a] (cm^2/cm^3)
Hydrated portland cement	1.53	0.0014	0.43	220×10^4
Normal weight concrete autoclaved	2.05	0.0027	0.24	10×10^4
Lightweight concrete 1, expanded shale	1.22	0.0010	0.34	90×10^4
Lightweight concrete 2, pumice	1.23	0.0010	0.39	
Clay brick	1.98	0.0025	0.26	10^4

[a]Estimated with assistance from Harmathy (31).

Cammerer (43) expressed the increase in the thermal conductivity as a unique function of the moisture concentration. There is a special case, that of steady-state heat conduction occurring during the capillary state, in which moisture in the porous solid can be regarded simply as a factor influencing the apparent value of thermal conductivity; and this value can be expressed as a function of moisture concentration (44).

Unfortunately, the concept of thermal conductivity as well-defined function of moisture concentration is not applicable to other conditions. In fact, even the assumption that thermal conductivity increases with increasing moisture concentration is questionable. If moisture flow takes a direction opposite that of heat flow, as is generally the

case in drying processes, the apparent value of the thermal conductivity of a solid in a moist condition is usually lower than that in the dry condition.

MOISTURE AND HEAT TRANSPORT IN CONCRETE

Although all that has been said in the previous sections about simultaneous moisture and heat transport in porous systems is applicable to concrete, concrete (or more specifically hydrated cement paste) has certain characteristics that make it different from most other inorganic porous materials.

A major portion of portland cement paste consists of an impure calcium silicate hydrate of somewhat indefinite composition, usually referred to as tobermorite gel. (There are some indications that it may not be entirely correct to regard portland cement paste as a gel.). This material has a very complex microstructure. It exhibits a specific surface that is unusually large among inorganic materials and surpassed only by industrial adsorbents. Consequently, portland cement paste can hold a substantial amount of moisture in equilibrium with a normal atmospheric environment (Fig. 1b). This implies that the critical point appears very early in the drying process, and that in the pendular state the moisture migration in cement paste is very slow. Figure 4 indicates the slowness of moisture migration in cement paste in comparison with that in a few other building materials. Although the thickness of the specimens was very small (1 cm), the temperature of the drying cabinet fairly high (41 C), and the water vapor concentration in the cabinet low, it took several days for the hydrated cement paste specimen to attain equilibrium with its surroundings.

Slowness of moisture movement in concrete, which sometimes appears to be a nuisance in technical problems, is more often a fortunate circumstance. Because of it, large concrete masses are capable of holding substantial amounts of capillary water in their central cores for long periods following placement, even under normal atmospheric conditions. Capillary water is essential for the hydration reactions that develop very slowly, often over several years. If the bulk of this capillary water is removed too early by the application of forced drying, the hydration reactions may stop completely (45) and the quality of the concrete suffers.

As one could expect by virtue of the Kozeny equation (32, 34), permeability of cement paste is very low. Because of this, high pressure gradients may develop in concrete structures if, in their capillary state, they are exposed to a sudden temperature rise. Under certain circumstances these pressure gradients may result in explosive spalling (46).

From a practical point of view, the progress of drying of concrete masses following placement is of particular interest, but unfortunately it is the most difficult to follow. Even for fully mature cement pastes, the capturing of water molecules by the solid matrix is not a simple surface phenomenon (adsorption). This fact always poses extra difficulties in defining sorption equilibria.

With fresh concretes the difficulties are augmented by the hydration reactions that continuously change the characteristics of the solid matrix and deplete the moisture participating in migration. Thus, for some time to come research workers concerned with the migration of moisture in fresh concrete structures will have to rely more on exploratory tests than on theoretical predictions.

NOMENCLATURE

The following symbols are used in the equations. Some symbols used as coefficients in Eq. 8 are not listed.

- C = constant in the Brunauer-Emmitt-Teller equation, dimensionless;
- D = effective coefficient of diffusion of water vapor in air inside a porous medium, cm^2/sec;
- g = gravitational acceleration, cm/sec^2;
- h = heat transfer coefficient, cal/cm^2 sec deg K;
- k = thermal conductivity of the porous system cal/cm sec deg K;
- K = capillary conductivity, sec;

ℓ = 1, 2;
L = thickness of slab, cm;
m = volumetric moisture concentration, cm^3/cm^3;
n = moisture flux, g/cm^2 sec;
P = total pressure, g/cm sec^2 (= $dyne/cm^2$);
P_v = equilibrium vapor pressure in the pores; partial pressure of water vapor in the environment, g/cm sec^2;
P_v° = equilibrium vapor pressure for free water, g/cm sec^2;
R = gas constant, g cm^2/sec^2 deg K mole;
s = specific surface, cm^2/cm^3;
t = time, sec (if not otherwise stated);
T = temperature, deg K (if not otherwise stated);
x = coordinate (horizontal), cm;
z = coordinate (vertical), cm;
α = mass transfer coefficient, mole/cm^2 sec;
ϵ = porosity, cm^3/cm^3;
$\varkappa$ = coefficient of capillary diffusion, cm^2/sec;
ν = empirical factor, dimensionless;
ρ = bulk density of solid matrix, g/cm^3;
ρ_m = density of moisture, g/cm^3;
Φ = total moisture potential, cm^2/sec^2;
φ = mole fraction of water vapor in the gaseous phase, mole/mole;
χ = coefficient of diffusion of moisture, cm^2/sec;
Ψ = capillary potential, cm^2/sec^2;
atm = atmospheric;
k = 1, 2, 3; and
∞ = of the ambient air.

ACKNOWLEDGMENT

The cooperation of E. Oracheski in the experimental work is greatly appreciated.

REFERENCES

1. Lewis, W. K. Ind. Eng. Chem., Vol. 13, 1921, p. 427.
2. Tuttle, F. Jour. Franklin Inst., Vol. 200, 1925, p. 609.
3. Sherwood, T. K. Ind. Eng. Chem., Vol. 21, No. 12, 1929, p. 976; Vol. 22, 1930, p. 132; Vol. 24, 1932, p. 307.
4. Newman, A. B. Trans. Amer. Inst. Chem. Eng., Vol. 27, No. 203, 1931, p. 310.
5. Childs, E. C. Jour. Agr. Sci., Vol. 26, No. 114, 1936, p. 527.
6. Kamei, S. Jour. Soc. Chem. Ind., Japan, Vol. 40, 1937, pp. 251, 257, 325, 366, 374.
7. Bird, R. B., Stewart, W. E., and Lightfoot, E. N. Transport Phenomena. Wiley, New York, 1960, p. 74.
8. McCready, D. W., and McCabe, W. L. Trans. Amer. Inst. Chem. Eng., Vol. 29, 1933, p. 131.
9. Hougen, O. A., McCauley, H. J., and Marshall, W. R., Jr. Trans. Amer. Inst. Chem. Eng., Vol. 36, 1940, p. 183.
10. Buckingham, E. Studies on the Movement of Soil Moisture. U.S. Dept. Agr., Bur. Soils Bull. 38, 1907.
11. Gardner, W. Soil Sci., Vol. 10, 1920, p. 357.
12. Israelson, O. W. Hilgardia, Vol. 2, 1927, p. 479.
13. Edlefsen, N. E., and Anderson, A. B. C. Hilgardia, Vol. 15, 1943, p. 31.
14. Richards, L. A. Physics, Vol. 1, 1931, p. 318.
15. Philip, J. R. Jour. Inst. Engrs., Australia, Vol. 26, 1954, p. 255.
16. Schofield, R. K. Trans. 3rd Internat. Congr. Soil Sci., Vol. 2, 1935, p. 37.
17. Philip, J. R. Proc. Natl. Acad. Sci., India, Vol. 24A, 1955, p. 93.

18. Philip, J. R. Soil Sci., Vol. 83, 1957, pp. 345, 435; Vol. 84, 1957, pp. 163, 257, 329; Vol. 85, 1958, pp. 278, 333.
19. Philip, J. R. Physics of Water Movement in Porous Solids. HRB Spec. Rept. 40, 1958, p. 147.
20. Philip, J. R., and de Vries, D. A. Trans. Amer. Geophys. Union, Vol. 38, 1957, p. 222.
21. de Vries, D. A. Trans. Amer. Geophys. Union, Vol. 39, 1958, p. 909.
22. Krischer, O. VDI Forschungsh, Vol. 415, 1942, p. 1.
23. Krischer, O. Die wissenschaftlichen Grundlagen der Trocknungstechnik. Springer-Verlag, Berlin, 1956.
24. Lykov, A. V., and Mykhaylov, Y. A. Theory of Energy and Mass Transfer. Prentice-Hall, Englewood Cliffs, N. J., 1961.
25. Lebedev, P. D. Internat. Jour. Heat Mass Transfer, Vol. 1, 1961, p. 294.
26. Haines, W. B. Jour. Agr. Sci., Vol. 16, 1927, p. 265; Vol. 20, 1930, p. 97.
27. Ceaglske, N. H., and Hougen, O. A. Trans. Amer. Inst. Chem. Eng., Vol. 33, 1937, p. 283.
28. Pearse, J. F., Oliver, T. R., and Newitt, D. M. Trans. Inst. Chem. Eng., Vol. 27, 1949, p. 1.
29. Corben, R. W., and Newitt, D. M. Trans. Inst. Chem. Eng., Vol. 33, 1955, p. 52.
30. Brunauer, S., Emmett, P. H., and Teller, E. Jour. Amer. Chem. Soc., Vol. 60, 1938, p. 309.
31. Harmathy, T. Z. Moisture Sorption of Building Materials. National Research Council, Canada, NRC 9492, 1967.
32. Harmathy, T. Z. Simultaner Feuchtigkeits-und Wärmetransport in porigen Systemen mit besonderem Hinweis auf Trocknung. Technische Hochschule, Wien, doctorial dissertation, 1967.
33. Feldman, R. F., and Sereda, P. J. Matériaux et Constructions, Vol. 1, 1968, p. 509.
34. Kozeny, J. S.-Ber. Akad. Wissensch, Wien, Vol. 136, 1927, p. 271.
35. Bouyoucos, G. J. Jour. Agric. Res., Vol. 5, 1915, p. 141.
36. Vassilou, B., and White, J. Trans. Ceram. Soc., Vol. 47, 1948, p. 351.
37. Paxton, J. A., and Hutcheon, N. B. Trans. ASHVE, Vol. 58, 1952, p. 301.
38. Gurr, C. G., Marshall, T. J., and Hutton, J. T. Soil Sci., Vol. 74, 1952, p. 335.
39. Hutcheon, W. L. Moisture Flow Induced by Thermal Gradients Within Unsaturated Soils. HRB Spec. Rept. 40, 1958, p. 113.
40. Kuzmak, J. M., and Sereda, P. J. Soil Sci., Vol. 84, 1957, p. 419.
41. Harmathy, T. Z. I&EC Fundamentals, Vol. 8, 1969, p. 92.
42. Collins, R. E. Flow of Fluids Through Porous Materials. Reinhold, New York, 1961.
43. Cammerer, J. S. Wärme-u. Kältetech., Vol. 41, 1939, p. 126.
44. Krischer, O., and Rohnalter, H. VDI Forschungsh., Vol. 402, No. 11B, 1940, p. 1.
45. Copeland, L. E., and Bragg, R. H. ASTM Bull. 204, Feb. 1955, p. 34.
46. Harmathy, T. Z. ASTM Spec. Tech. Publ. 385, 1965, p. 74.

A Review of Methods for Measuring Water Content of Highway Components in Place

G. E. MONFORE, Portland Cement Association, Skokie, Illinois

A discussion of the kinds of water that may be present in porous materials, and their importance to various physical properties, is followed by a description of several instruments that have been suggested for measuring water content. The principle of each method of measurement is outlined and some factors of importance in the application of the methods to highway materials are mentioned. Further information on details of the instruments and their use may be found in the references cited in the text.

THIS review includes methods that have been or might be used for measuring the water content of porous materials found in highway components, such as structures, pavements, base courses, or subgrades. Most of the literature on the subject is concerned with concrete or soils.

A comprehensive review was not attempted because of the vast amount of literature involved. For example, a bibliography (1) published in 1959 contains 629 references to methods for determining water content of soils, and other publications describing methods for measuring water contents of various materials (2), solids (3), building materials (4, 5), and soils using nuclear devices (6, 7) contain an additional 930 references.

Costs of the various types of equipment are not considered here, but Roth (8) gives cost ranges in 1966 for some types of instruments. Smith et al. (7) gives manufacturers of nuclear instruments available in 1963.

AMOUNTS AND KINDS OF WATER IN POROUS MATERIALS

Before various instruments that may be used for measuring water contents of porous materials are discussed, some background information on the amounts and kinds of water usually found in such materials is desirable.

Water in porous materials may be fixed to the solid phase in various degrees, ranging from chemically bound to essentially unbound or free. For instance, in hardened portland cement paste, the "solid" material results from the chemical reaction of portland cement with about 23 percent water by weight of the dry cement (9, p. 975). This water is chemically bound and its removal drastically changes the properties of the solid. This solid is a porous solid containing minute pores, called gel pores, and larger pores, called capillary pores. Water in the gel pores is bound by adsorptive forces, i.e., by physical attractions between the molecules at the surface of the solid and water molecules. The capillary water is also under the influence of surface forces but is not as tightly bound as the gel water. Gel water and capillary water may be removed and reabsorbed without drastic changes occurring in the properties of the material. Chemically bound water, gel water, and capillary water in hardened portland cement paste do not form discrete groups that are readily separated, but rather form a more or less continuous spectrum. For this reason water in hardened paste is conveniently divided into evaporable and nonevaporable water (9, p. 252). Nonevaporable water approximates the chemically bound water, and evaporable water approximates the sum of gel

Paper sponsored by Committee on Performance of Concrete—Physical Aspects and presented at the 49th Annual Meeting.

and capillary water. Evaporable water is customarily defined as that which is removed under a vacuum of 0.5 micron of mercury at 23 C (10). This corresponds approximately to the water lost during drying in an oven at 105 C.

Soils may also contain appreciable amounts of nonevaporable water. The evaporable water in soils, however, is generally bound less tightly than that in hardened portland cement paste, and is frequently classified as hygroscopic, capillary, and gravitational (11). Hygroscopic water and capillary water are under the influence of surface forces, while gravitational water is the part that will drain from a soil under the force of gravity.

Evaporable water content is usually expressed as a percentage of the oven-dry (105 C) weight of the material, and this procedure will usually be followed in the present paper. It should be noted, however, that some literature references do not specifically state the basis for expressing water content.

Considerable data are available on nonevaporable water contents of hardened portland cement pastes, but few data were found for soils and aggregates. Information that was available is given in Table 1. It should be noted that aggregates, concretes, and soils may contain appreciable amounts of nonevaporable water.

Evaporable water contents of highway materials in a saturated condition are given in Table 2; it is worthy of note that the evaporable water contents are variable and may be considerable for some materials.

As might be expected, various physical properties of porous materials are influenced by the amounts and kinds of water in the materials. Some properties are a function primarily of one kind of water, while other properties are influenced by more than one kind. For example, the strength of normal-weight concrete is primarily a function of the nonevaporable water in the paste. By contrast, drying shrinkage of concrete under outdoor conditions is primarily a function of the evaporable water, both in the paste and in the aggregate. The amount of water in concrete that will freeze under outdoor winter conditions may be about one-third of the saturated evaporable water content (19). The behavior of the concrete as ice forms will be influenced by the strength, which is, as

TABLE 1

NONEVAPORABLE WATER CONTENTS

Material	Nonevaporable Water, Percent Dry Weight (above 100-110 C)	
	Range	Average
Aggregates (13)		
Andesites	0.5-2.2	
Basalts	0.4-1.5	
Diabases	1.0-2.8	
Diorites	0.4-2.4	
Gabbros	0.4-2.4	
Gneisses	0.4-1.6	
Granites	0.3-0.9	
Igneous, 1800 specimens		1.4
Limestones, 345 specimens		0.6
Quartz porphyry	0.6-1.0	
Rhyolites	0.2-4.5	
Sandstones	0.2-2.2	
Sandstones, 253 specimens		1.3
Schists	0.7-4.6	
Serpentines	10.5-23.9	
Shales	2.1-6.8	
Slates	2.8-4.1	
Concrete[a]	3.4-5.7	
Petroleum asphalts (14)	7-11 (hydrogen content)	
Portland cement paste, hardened		18
Soils		
Clays (13, 15, 16)	6.2-14.1	
Silt (13)		2.0

[a]Assuming 520 lb cement per cu yd, 0.5 water-cement ratio, 6 percent air, and 0.2 to 3 percent nonevaporable water in the aggregate.

TABLE 2

EVAPORABLE WATER CONTENTS OF SATURATED MATERIALS

Material	Evaporable Water, Percent Dry Weight (up to 100-110 C)	
	Range	Average
Aggregates (17)		
Basalts	0.0-3.5	0.5
Cherts	0.1-8.9	1.6
Diabases	0.0-4.2	0.3
Diorites	0.0-1.8	0.3
Dolomites	0.0-9.0	1.1
Felsites[a]	0.0-5.3	0.8
Gabbros	0.0-1.1	0.3
Gneisses	0.0-2.4	0.3
Granites	0.0-1.9	0.3
Limestones	0.0-17.8	0.9
Quartzites	0.0-1.9	0.3
Sandstones	0.1-19.9	1.8
Schists	0.0-2.7	0.4
Serpentines	0.0-3.8	0.9
Slates	0.1-4.3	0.5
Concrete[b]	4.8-8.8	
Petroleum asphalts (18)	0-0.5	
Portland cement paste, hardened[c]		27
Soils (19)	8-24	

[a]Includes andesites, dacites, rhyolites, and trachytes.
[b]Assuming 520 lb cement per cu yd, 0.5 water-cement ratio, 6 percent air, and 0.1 to 5 percent evaporable water in the aggregate.
[c]0.5 water-cement ratio.

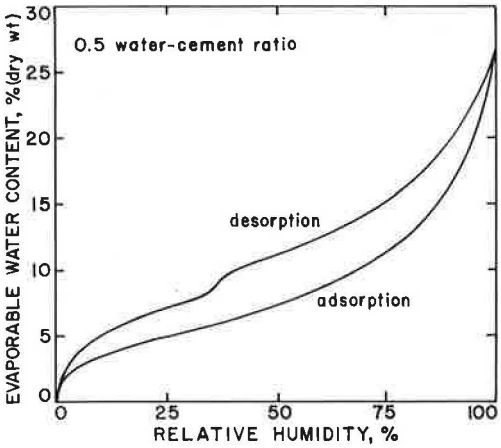

Figure 1. Sorption isotherms for hardened portland cement paste (21).

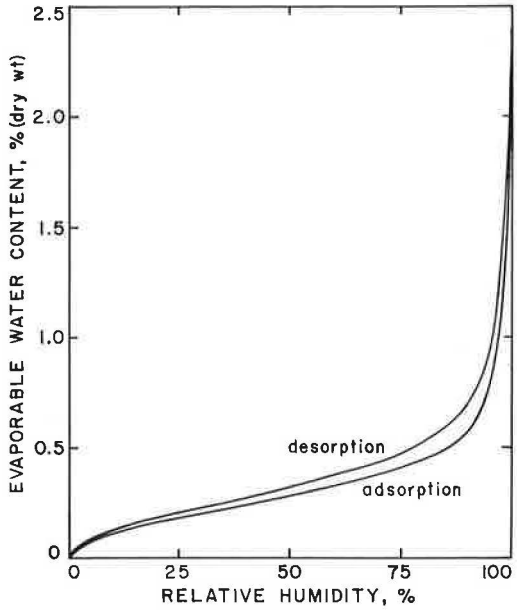

Figure 2. Sorption isotherms for a graywacke (22).

previously noted, primarily a function of the nonevaporable water content of the paste. Thus, the response of concrete to freezing is affected by both evaporable and nonevaporable water.

The exchange of water between a porous material and the surrounding atmosphere depends on the vapor pressures of the water in the two locations, with movement being from a region of higher pressure toward a region of lower pressure. The evaporable water in porous materials is bound in various degrees by forces originating in the surface of the solid phase. As a consequence of these surface forces, the vapor pressure of evaporable water in porous materials averages less than that of bulk water, but may range from essentially that of bulk water to very low values for water in minute pores, such as gel pores in cement paste.

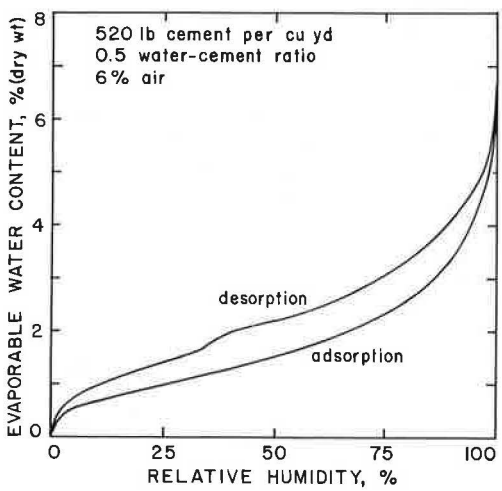

Figure 3. Calculated sorptions isotherms for a concrete.

Evaporable water contents of porous materials can thus be related to the vapor pressure of the water. It is usually more convenient, however, to relate evaporable water content to the relative humidity (ratio of actual vapor pressure to vapor pressure at saturation) of an atmosphere that is in equilibrium with the porous material. These relationships at constant temperature are known as sorption isotherms. Such curves for a hydrated portland cement paste (20) are shown in Figure 1. Notice that the relation as water is added to the paste (adsorption isotherm) differs from that when water is extracted (desorption isotherm). This hysteresis effect is found in some degree in all porous materials. Figure 2 shows sorption curves for a particular aggregate (21), and the curves of Figure 3 for concrete were computed from the relationships of Figures 1 and 2. The evaporable water content of this concrete from 0 to about 4.5 percent is seen to be adequately differentiated

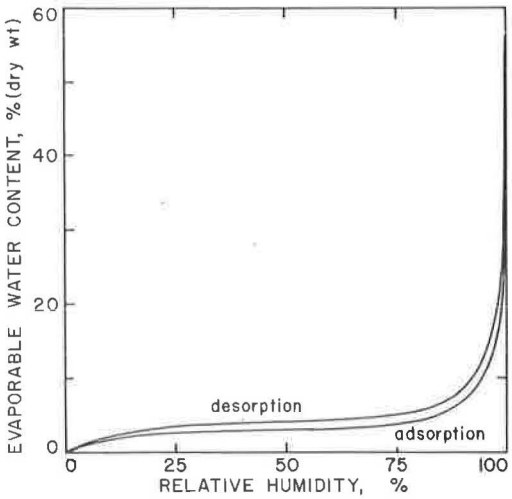

Figure 4. Sorptions isotherms for a clay (23).

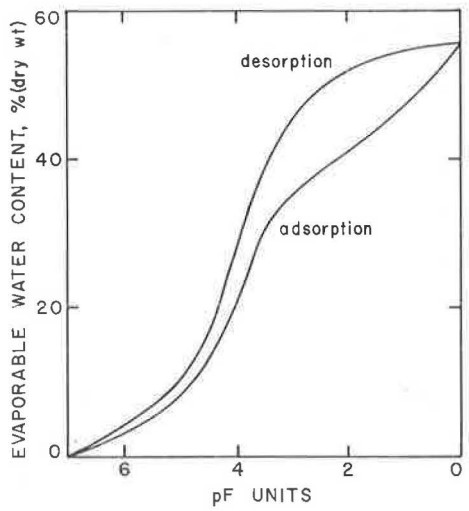

Figure 5. Water content versus pF units for a clay (23).

by relative humidity that varied from 0 to 95 percent. However, above 95 percent relative humidity the curves are very steep and, hence, in this region relative humidity is not a sensitive measure of water content.

The sorption curves for most soils are even steeper in the region of high relative humidity (Fig. 4). More than half of the evaporable water in this clay (22) was adsorbed between 99 and 100 percent relative humidity. Because of this insensitivity of relative humidity in the region of high water contents of soils, and also for other reasons, soil scientists have adopted another measure that is more convenient. Reduced vapor pressure in porous materials may be related to the height of water in a capillary tube having the same vapor pressure. Logarithms of these heights of water columns in capillary tubes, measured in cm, are known as pF units (23, 24). The utility of pF units for soils is apparent when the data of Figure 4 are replotted (Fig. 5) using the corresponding pF units.

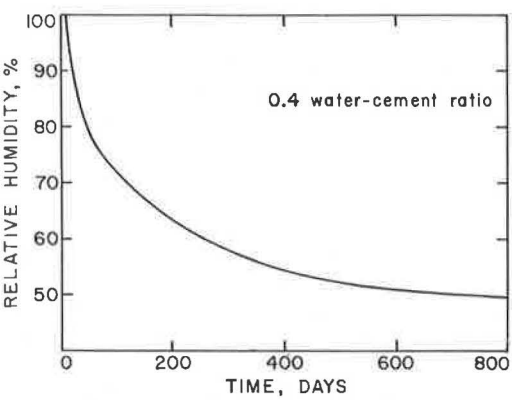

Figure 6. Relative humidity on axis of 3- by 6-in. mortar cylinder (26).

The rate at which water is transferred from porous materials to the surrounding atmosphere, especially the rate of drying of concrete, is of interest in highway applications. Figure 6, for instance, shows the relative humidity in a small cavity located on the axis of a 3- by 6-in. mortar cylinder (25) as a function of drying time in an atmosphere of 50 percent relative humidity and 73 F. The mortar consisted of 1 part cement, 0.4 part water, 2.85 parts Ottawa sand, and was fog-cured 7 days before drying. Although the water had to travel only 1.5 in. from the axis of the cylinder to the surface, two years were required to reach equilibrium conditions. At the conclusion of the drying period, when the relative humidity of the cylinder was 50 percent, the cylinder was submerged in water. After 24 hours in

water, the relative humidity on the axis of the cylinder had increased from 50 to 98 percent. Thus, mortar or concrete loses water very slowly when exposed to a drying atmosphere, but gains water rapidly when subjected to liquid water.

MEASUREMENT OF WATER IN POROUS MATERIALS

Several methods for measuring water contents of porous materials are briefly outlined. A statement of the principle involved in each method is followed by a discussion of the applicability to highway components. Advantages and disadvantages of the several methods depend on the material and the property of the material under investigation. For example, if freezing phenomena are of prime interest, the method should measure the freezable water, i.e., the less tightly bound evaporable water; if drying shrinkage of concrete is the main concern, the method should measure the more tightly bound evaporable water. Some methods measure evaporable water only, while others measure total water, evaporable plus nonevaporable.

Relative Humidity Methods

There are many methods for measuring the relative humidity of an atmosphere, but only a few are applicable for use in a small cavity inside a porous material. These latter methods depend on the measurement of a property of some sensor in moisture equilibrium with the atmosphere in the cavity, such as electrical resistance of a film containing lithium chloride (26, 27, 28), capacitance of an aluminum oxide film (29, 30), length change of wood (31), length change of a polyester thread (25, 32), or electrical resistance of a gypsum block (33, 34).

These methods measure changes related to the evaporable water content of the porous materials. If the amount of evaporable water is needed, calibration curves, such as those in Figures 3 or 4, for the material under study are necessary. However, for some applications, relative humidity in the material may be related directly to other properties, such as drying shrinkage of concrete. In evaluating relative humidity methods, the range of water contents of interest, hysteresis effects both in the material and in the sensitive element, and size of the sensitive element should be considered.

There are probably no relative humidity instruments sufficiently stable to give accurate readings over long periods of time without periodic calibration. The use of relative humidity wells is thus indicated (25). The instrument may then be placed in the well only when relative humidity measurements are made.

Thermal Conductivity Methods

The thermal conductivity of porous materials increases with increase in water content; thus, physical measurements that are related to thermal conductivity may be used to measure water content. The usual method is to heat a slender probe by means of an electric current and to measure the rate at which the temperature of the probe increases. The higher the water content of the surrounding material, the faster the heat is conducted away and the slower the temperature rise. Various modifications have been suggested, including the use of a copper wire as heater and temperature detector (35), a thermocouple as temperature detector (36), a series of thermocouples to measure moisture gradients (37), and a thermistor as temperature detector (38).

Calibration of the instrument with each material to be studied is necessary, and may be done in terms of evaporable water content. An important factor in the practical use of thermal conductivity devices is obtaining proper thermal contact between probe and porous material.

Resistance Methods

Electrical resistance methods were used as early as 1897 in soils (39) and 1938 in concrete (40) for the estimation of water content. Direct measurement of the resistance between two electrodes embedded in a porous material, however, is subject to errors due to variable contact resistance between electrodes and material and to errors due to variations in concentration of soluble salts (41). Such errors may be lessened by

embedding the electrodes in a material, such as gypsum (42), and then embedding the gypsum block in the porous material to be studied. Although both gypsum and soils or concretes in which the gypsum block is embedded exhibit hysteresis effects, the evaporable water content of the soil or concrete may be calibrated in terms of the electrical resistance of the gypsum block. Nylon, fiberglass, and combinations of these materials with gypsum (43, 44), aluminous cement (45), and portland cement mortar (46) have been suggested as materials for absorbent blocks in combination with various metals for electrodes. Another modification suggested to lessen the contact resistance error is that of using four electrodes instead of the usual two electrodes (47, 48).

The electrical resistance of concrete subject to low frequency alternating current is a function of the evaporable water content (49); the resistance of soils would likewise be expected to depend on evaporable water content.

Capacitance Methods

The dielectric constant of water is about 80 and is relatively insensitive to changes in temperature from 15 to 35 C and to changes in frequency from 10^5 to 3×10^8 Hz. Furthermore, addition of sodium chloride in amounts from 0.1 to 0.7 mole has little effect (50). The dielectric constant of oven-dry soils (51) is only about 2.6; thus, the addition of water to soils should cause a significant increase in the dielectric constant. Capacitance methods are accordingly very attractive from a theoretical view, and several publications describe such equipment (41, 51, 52, 53). One investigator (51), using stainless steel electrodes directly in soils and a frequency of 3×10^7 Hz, reported that the relationship between water content expressed on a volume basis and capacitance was independent of the type of soil and the presence of 0.2 percent sodium chloride in the water. Others (41, 53) using gypsum blocks in soils and concrete between insulated electrodes found capacitance to be influenced by the presence of sodium chloride in the water.

Microwave-Absorption Methods

Another method that has been used for determination of water content is abosrption of electromagnetic radiation by the material. Such absorption is a function of the dielectric constant (54, 55, 56) and is thus closely related to capacitance methods (51).

Measurements are made by determining the attenuation of the radiation as it passes from the transmitting horn antenna through the specimen to the receiving horn antenna. Wavelengths of 3 cm (10^{10} Hz) and 10 cm (3×10^9 Hz) have been used for such studies (57, 58). The relation between evaporable water content on a volume basis and absorption of microwaves was found to be linear (57, 58) but varied with the material. Thus, calibration with the particular material under study is necessary.

Neutron-Scattering Methods

Fast neutrons penetrating a material are subject primarily to two reactions, scattering and absorption. Scattering is the result of elastic collisions between neutrons and atomic nuclei of the material, and absorption is the inelastic reaction in which the neutrons enter the nuclei and produce new nuclei species. When neutrons collide with nuclei, they lose energy and eventually are slowed down until their kinetic energy approaches the thermal kinetic energy of the surrounding atoms. Energy loss on collision is greatest when the two colliding particles have the same mass; hence, hydrogen nuclei, having essentially the same mass as neutrons, are the most efficient of all atomic nuclei in reducing the velocity of neutrons. Thus, if a source of high-energy neutrons and a detector of low-energy or thermal neutrons are placed in a hole in a material, or are placed side by side on a surface of a material, the number of neutrons that are reduced to thermal energies and diffuse back to the detector will be largely a function of the number of hydrogen nuclei in the vicinity. This is the principle of neutron-scattering methods for determining moisture contents of porous materials. The literature on such devices is vast and only a few references can be mentioned here. Earlier work is reviewed (59, 60, 61), while later work is summarized (6, 7, 62, 63).

If the number of thermal neutrons produced when a material is irradiated with fast neutrons were solely a function of hydrogen concentration, a single calibration curve could be used for all materials. However, it has been shown experimentally (64, 65, 66, 67) and demonstrated theoretically (62, 63, 67, 68) that scattering by other atomic nuclei and absorption losses are not negligible, and therefore a single calibration curve cannot be used for all materials. Accordingly, considerable effort has been directed toward methods for calibrating neutron meters (63, 64, 65, 69, 70). The volume of material that influences the thermal neutron flux near subsurface gages depends on the water content, and was reported (7) to vary in radius from 4 to 18 in. and in thickness from 4 to 24 in. These large spheres of influence make calibration in soils in place very difficult, and accordingly most efforts toward calibration procedures have been directed toward development of laboratory methods.

The effect of differences in composition of the material on neutron-scattering results may be lessened by use of a cadmium shield (71) over the detector, but such a shield drastically reduces the number of thermal neutrons available for counting.

Because asphalts contain relatively large amounts of hydrogen (Table 1), neutron-scattering methods have been suggested (72) for the determination of the asphalt contents of asphaltic concretes.

It should be re-emphasized that neutron-scattering methods do not distinguish between evaporable and nonevaporable water.

SUMMARY AND CONCLUSIONS

The water content of highway materials, such as concretes, aggregates, and soils, may be conveniently divided into evaporable water, which is that lost during drying in an oven at about 105 C, and nonevaporable water, which is lost only at temperatures higher than 105 C. It will be noted from Table 1 that the amounts of nonevaporable water in highway materials may be considerable.

Physical properties of highway materials are influenced in various degrees by the amounts and kinds of water present; thus, the selection of a method for measuring water content depends on the physical property that is of prime interest. If this should be action under freezing conditions, then the amount of freezable water is the important water content to be measured; and for some materials this may be only a small part of the evaporable water.

Neutron-scattering methods are sensitive to total water content, whereas all of the other methods discussed here may be used to measure evaporable water.

Equilibrium relative humidity methods are simple, and calibration of the instruments in terms of relative humidity is independent of the material to be investigated. However, to obtain evaporable water contents, relationships between relative humidity and evaporable water content must be determined, and these relationships depend on the material. Also at high evaporable water contents, particularly in soils, relative humidity instruments are insensitive.

All methods, except that of equilibrium relative humidity, depend on composition and density of the material under study; hence, calibrations are necessary.

Thermal conductivity, resistance, and capacitance methods are susceptible to changes in the contact between the instruments and the porous materials, particularly over long periods of time. Soluble salts in the water may influence resistance and capacitance measurements.

Microwave-absorption methods are presently limited to specimens that may be interposed between the transmitter and the receiver and are, thus, of limited use in highway components.

Neutron-scattering methods sample large volumes of the material, which may be an advantage in some applications, but accordingly are not useful for measurement of moisture gradients. If evaporable water contents are of interest, they must be obtained by subtracting the measured or estimated nonevaporable water content from the total water content that is obtained by the neutron instrument.

There is no instrument that is satisfactory for measuring the water contents of highway materials that may be important to the behavior of these materials under all conditions.

REFERENCES

1. Shaw, M. D., and Arble, W. C. Bibliography on Methods for Determining Soil Moisture. College of Engineering and Architecture, Pennsylvania State Univ., University Park, Eng. Res. Bull. B-78, 1959, 152 pp.
2. Schedule and Abstract of Technical Papers. 1963 Internat. Symposium on Humidity and Moisture, Washington, D. C., 1963.
3. Geary, P. J. Determination of Moisture in Solids: A Short Survey of Methods and Apparatus. British Scientific Instrument Research Assn., Res. Rept. M-24, 1956, 52 pp.
4. Methods and Apparatus for the Measurement of Humidity in Building Materials. RILEM, Bull. 15, 1962, 197 pp.
5. In Situ Measurement of Moisture. RILEM/CIB Symposium on Moisture Problems in Building, Helsinki, Vol. 2, Section 6, 1965, 201 pp.
6. Use of Neutron Meters in Soil Moisture Measurements. Proc. ASCE, Vol. 90, No. HY6, Nov. 1964, pp. 21-43; Vol. 92, No. HY3, May 1966, pp. 72-75.
7. Smith, P. C., Johnson, A. I., Fisher, C. P., and Womack, L. M. Use of Nuclear Meters in Soils Investigations: A Summary of World-Wide Research and Practice. ASTM, STP 412, 1968, 136 pp.
8. Roth, M. How to Measure Moisture in Solids. Chemical Engineering, Vol. 73, 1966, pp. 83-88.
9. Powers, T. C., and Brownyard, T. L. Studies of the Physical Properties of Hardened Portland Cement Paste. Research Dept., Portland Cement Assn., Skokie, Ill., Bull. 22, 1948.
10. Copeland, L. E., and Hayes, J. C. The Determination of Non-Evaporable Water in Hardened Portland Cement Paste. Research Dept., Portland Cement Assn., Skokie, Ill., Bull. 47, 1953.
11. Karol, R. H. Soils and Soil Engineering. Prentice-Hall, New York, 1960, p. 8.
12. Clarke, F. W. Data of Geochemistry. U. S. Geological Survey Bull. 770, 1924.
13. Kirk-Othmer Encyclopedia of Chemical Technology, 2nd Ed. Interscience Publishers, Vol. 2, 1963, p. 787.
14. Caldwell, A. C., and Rost, C. D. The Chemical Composition of the Clay Fractions of the Black Prairie Soils of Minnesota. Soil Science, Vol. 53, 1942, p. 249.
15. Lyon, T. L., and Buckman, H. D. The Nature and Properties of Soils. Macmillan, New York, 1949, p. 77.
16. Woolf, D. O. Results of Physical Tests of Road-Building Aggregates. U. S. Bureau of Public Roads, 1953.
17. The Asphalt Handbook. The Asphalt Institute, 1967, pp. 58-60.
18. Hewes, L. I., and Oglesby, C. H. Highway Engineering. John Wiley and Sons, New York, 1954, p. 326.
19. Verbeck, G. J., and Klieger, P. Calorimeter-Strain Apparatus for Study of Freezing and Thawing Concrete. Research Dept., Portland Cement Assn., Skokie, Ill., Bull. 95, 1958.
20. Sereda, P. J., Feldman, R. F., and Swenson, E. G. Effect of Sorbed Water on Some Mechanical Properties of Hydrated Portland Cement Pastes and Compacts. Symposium on Structure of Portland Cement Paste and Concrete, HRB Spec. Rept. 90, 1966, p. 69.
21. Verbeck, G. J., and Landgren, R. Influence of Physical Characteristics of Aggregates on Frost Resistance of Concrete. Research Dept., Portland Cement Assn., Skokie, Ill., Bull. 126, 1960.
22. Penner, E. Electrical Resistance Meters for Soil Moisture Measurements. RILEM, Bull. 15, 1962, p. 99.
23. Schofield, R. K. The pF of Water in the Soils. Trans. Third Internat. Congress of Soil Science, Vol. 2, 1935, pp. 37-48.
24. Sereda, P. J., and Hutcheon, N. B. Moisture Equilibrium and Migration in Building Materials. ASTM, STP 385, 1964, pp. 3-7.
25. Monfore, G. E. A Small Probe-Type Gage for Measuring Relative Humidity. Research Dept., Portland Cement Assn., Skokie, Ill., Bull. 160, 1963.

26. Dunmore, F. W. An Improved Electrical Hygrometer. Jour. of Research: Eng. and Instrumentation, Vol. 23, 1939, pp. 701-714.
27. Gause, G. R., and Tucker, J. Method for Determining the Moisture Content in Hardened Concrete. Journal of Research: Eng. and Instrumentation, Vol. 25, 1940, pp. 403-416.
28. Handegord, G. O., Hedlin, C. P., and Trofimenkoff, F. N. A Study of the Accuracy of Dunmore Type Humidity Sensors. Internat. Symposium on Humidity and Moisture, Washington, D. C., Paper C4.1.3, 1963.
29. Cutting, C. L., Jason, A. C., and Wood, J. L. A Capacitance-Resistance Hygrometer. Jour. Scientific Instruments, Vol. 32, 1955, pp. 425-431.
30. Jason, A. C. Some Properties and Limitations of the Aluminum Oxide Hygrometer. Internat. Symposium on Humidity and Moisture, Washington, D. C., Paper C4.3.1, 1963.
31. DeCastro, E. Vibrating Wire Tele-Hygrometers for "In Situ" Determination of Moisture Content. RILEM, Bull. 15, 1962, pp. 155-195.
32. Abrams, M. S., and Monfore, G. E. Application of a Small Probe-Type Relative Humidity Gage to Research on Fire Resistance of Concrete. Research Dept., Portland Cement Assn., Skokie, Ill., Bull. 186, 1965.
33. Bouyoucos, G. J., and Cook, R. L. Humidity Sensor. Permanent Electric Hygrometer for Continuous Measurement of the Relative Humidity of the Air. RILEM/CIB Symposium on Moisture Problems in Building, Helsinki, Vol. 2, Section 6, Paper 6-2, 1965.
34. Nielsen, K. E. C. Measurement of Water Vapor Pressure in Hardened Concrete. Swedish Cement and Conc. Res. Inst., Stockholm, Bull. 35, 1967.
35. Shaw, B., and Baver, L. D. An Electrothermal Method for Following Moisture Changes of the Soil in Situ. Soil Sci. Soc. Amer., Proc. Vol. 4, 1939, pp. 78-83.
36. DeVries, D. A. A Nonstationary Method for Determining Thermal Conductivity of Soil in Situ. Soil Science, Vol. 73, 1952, pp. 83-89.
37. Vos, B. H. Measurements of Moisture Content in Building Structures in Situ. RILEM/CIB Symposium on Moisture Problems in Building, Helsinki, Vol. 2, Section 6, Paper 6-1, 1965.
38. Globus, A. M., and Kaganov, M. A. A Portable Device and Probe for the Measurement of Moisture Content and Temperature of Capillary Porous Materials. RILEM/CIB Symposium on Moisture Problems in Building, Helsinki, Vol. 2, Section 6, Paper 6-11, 1965.
39. Whitney, M., Gardner, F. D., and Briggs, L. J. An Electrical Method of Determining the Moisture Content of Arable Soils. U. S. Dept. of Agr., Div. of Soils Bull. 6, 1897.
40. Spencer, R. W. Measurement of the Moisture Content of Concrete. Proc. ACI, Vol. 34, 1938, pp. 45-61.
41. Hancox, N. L., and Walker, J. The Influence of Liquid Resistivity Changes on Plaster of Paris Resistance and Capacitance Moisture Gauges. British Jour. of Appl. Physics, Vol. 17, 1966, pp. 827-833.
42. Bouyoucos, G. J., and Mick, A. H. An Electrical Resistance Method for Continuous Measurement of Soil Moisture Under Field Conditions. Michigan Agr. Exp. Sta. Tech. Bull. 172, 1940.
43. Olson, D. F., and Hoover, M. D. Methods of Soil Moisture Determination Under Field Conditions. U. S. Dept. of Agr., Southeastern Forest Exp. Sta., Asheville, N. C., Paper 38, pp. 10-16.
44. Bourget, S. J., Elrick, D. E., and Tanner, C. B. Electrical Resistance Units for Moisture Measurements: Their Moisture Hysteresis, Uniformity, and Sensitivity. Soil Science, Vol. 86, 1958, pp. 298-304.
45. Croney, D., Coleman, J. D., and Bridge, P. M. The Suction of Moisture Held in Soil and Other Porous Materials. U. K. Dept. of Sci. and Ind. Research, Road Research Tech. Paper 24, 1952, pp. 38-41.
46. Mertin, W. Method of Measuring the Distribution of Moisture in Concrete and Reinforced Concrete Structures. RILEM/CIB Symposium on Moisture Problems in Building, Helsinki, Vol. 2, Section 6, Paper 6-9, 1965.

47. McCorkle, W. H. Determination of Soil Moisture by the Method of Multiple Electrodes. Texas Agr. Exp. Sta. Bull. 426, 1931.
48. Ressurreicao Neto, J. M. Moisture Content in Earth Structures: Its Determination "In Situ". RILEM, Bull. 15, pp. 47-56, 1962.
49. Monfore, G. E. The Electrical Resistivity of Concrete. Research Dept., Portland Cement Assn., Skokie, Ill., Bull. 224, 1968.
50. Von Heppel, A. R. Dielectric Materials and Applications. John Wiley and Sons, New York, 1954, p. 361.
51. Thomas, A. M. In Situ Measurement of Moisture in Soil and Similar Substances by Fringe Capacitance. Jour. Sci. Instruments, Vol. 43, 1966, pp. 21-27.
52. Anderson, A. B. C., and Edlefsen, N. E. The Electrical Capacity of the 2-Electrode Plaster-of-Paris Block as an Indicator of Soil Moisture Content. Soil Science, Vol. 54, 1942, pp. 35-46.
53. Bell, J. R., Leonards, G. A., and Dolch, W. L. Determination of Moisture Content of Hardened Concrete by Its Dielectric Properties. Proc. ASTM, Vol. 63, 1963, pp. 996-1007.
54. Hasted, J. B., and Edmonds, P. H. Microwave Absorption in Damp Brick. RILEM, Bull. 15, 1962, pp. 88-90.
55. Boot, A. R., and Watson, A. Applications of Centimetric Radio Waves in Non-Destructive Testing. Internat. Conf. on Materials, ASTM, 1964, pp. 1-35.
56. Hasted, J. B., and Shah, M. A. Microwave Absorption by Water in Building Materials. British Jour. Appl. Physics, Vol. 15, 1964, pp. 825-836.
57. Mathey, R. The Application of Electromagnetic Radiation to the Investigation of the Moisture Content of Materials. RILEM, Bull. 15, 1962, pp. 138-143.
58. U. K. Dept. of Sci. and Ind. Research. The Non-Destructive Measurement of Water Content by Micro-Wave Absorption: Further Developments. RILEM, Bull. 15, 1962, pp. 85-87.
59. Pawliw, J., and Spinks, J. W. T. Neutron Moisture Meter for Concrete. Canadian Jour. of Tech., Vol. 34, 1957, pp. 503-513.
60. Roy, S. E., and Winterkorn, H. F. Scintillation Methods for the Determination of Density and Moisture Content of Soils and Similar Granular Systems. HRB Bull. 159, 1957, pp. 58-135.
61. Symposium on Nuclear Methods for Measuring Soil Density and Moisture. ASTM, STP 293, 1960.
62. Ballard, L. F., and Gardner, R. P. Density and Moisture Content Measurements by Nuclear Methods. NCHRP Rept. 14, 1965, pp. 21-30.
63. Gardner, R. P., and Roberts, K. F. Density and Moisture Content Measurements by Nuclear Methods. NCHRP Rept. 43, 1967, pp. 20-30.
64. Burn, K. N. A Neutron Meter for Measuring Moisture in Soils. RILEM, Bull. 15, 1962, pp. 91-92.
65. Burn, K. N. Calibration of a Neutron Soil Moisture Meter. Internat. Symposium on Humidity and Moisture, Washington, D. C., Paper D3.7, 1965.
66. Waters, E. H. Measurement of Moisture in Concrete and Masonry With Special Reference to Neutron Scattering Techniques. RILEM/CIB Symposium on Moisture Problems in Building, Helsinki, Vol. 2, Section 6, Paper 6-3, 1965.
67. Gemmell, W., McGregor, B., and Moss, G. F. Estimation of Moisture Content by Neutron Scattering: Theory, Calculation, and Experiment. Internat. Jour. of Appl. Radiation and Isotopes, Vol. 17, 1966, pp. 615-620.
68. Kasi, S., and Koskinen, H. Analysis, Calculations, and Measurements Concerning the Moisture Measuring by the Neutron Method. RILEM/CIB Symposium on Moisture Problems in Building, Helsinki, Vol. 2, Section 6, Paper 6-14, 1965.
69. Hughes, C. S., and Anday, M. C. Correlation and Conference of Portable Nuclear Density and Moisture Systems. Highway Research Record 177, 1967, pp. 239-257.
70. LeFevre, E. W., and Manke, P. G. A Tentative Calibration Procedure for Nuclear Depth Moisture/Density Gages. Highway Research Record 248, 1968, pp. 82-90.
71. Preiss, K., and Grant, P. J. The Optimization of a Neutron Scattering Water Content Gauge for Soils or Concretes. Jour. Sci. Instruments, Vol. 41, 1964, pp. 548-551.
72. Grey, R. L. Determination of Asphalt Content in Hot Bituminous Mixes With a Portable Nuclear Asphalt Content Gage. Highway Research Record 248, 1968, pp. 77-81.

Field and Laboratory Studies of the Effect of Subbase Type on the Development of D-Cracking

DAVID STARK, Portland Cement Association, Skokie, Illinois

Field and laboratory observations of numerous pavements have indicated that the development of D-cracking depends on the nature of the coarse aggregate used in the concrete and the facility with which moisture can be transported away from the subbase and pavement slab. It has been found necessary to install longitudinal tile subdrains in the shoulder areas to prevent the development of D-cracking associated with numerous coarse aggregates. Varying the type of subbase material also has been found to affect the rate of development of deterioration. Based on these observations, a series of simulated pavement slabs was cast in the PCA outdoor test plot to study the effect of granular, clay, cement-treated, and granular + vapor barrier subbases on moisture movements and the development of distress in the concrete slabs. Three coarse aggregates known to cause D-cracking were used. Moisture changes were based on weight measurements of 1-in. thick by 5½-in. diameter concrete discs tightly secured and inserted into precast cylindrical holes of similar size in each slab. Results after two freeze-thaw seasons showed that the level of saturation in all slabs had increased and, based on the examination of crack patterns in cores taken from the slab, certain particles of coarse aggregate had become critically saturated prior to freezing. It was also found necessary to take into consideration certain factors unique to the test procedure in the interpretation of the test results.

•DURING the past several years, field studies of a large number of pavements have revealed the widespread occurrence of a type of deterioration known as D-cracking, in which distress develops along joints, structural cracks, and the outside edges of pavement slabs (Fig. 1). Further observations revealed that deterioration was initiated in the lower levels of the pavement slab (Fig. 2). These observations and associated laboratory studies indicated that distress was due to the freeze-thaw failure of coarse aggregate particles (Fig. 3), and that pavement design, or the environment into which the concrete was placed, was a decisive factor in the durability of the pavement (1). Recognition of this fact led to studies at the PCA laboratories in which various combinations of subbases and concrete slabs were placed in an outdoor test plot to simulate pavement exposures in a freeze-thaw climate. It was anticipated that the findings in this study would indicate the need for durability as well as other considerations in pavement design. Additional information from the field observations, together with interim results from the laboratory tests, are discussed.

Paper sponsored by Committee on Performance of Concrete—Physical Aspects and presented at the 49th Annual Meeting.

Figure 1. D-cracking along transverse joint of pavement.

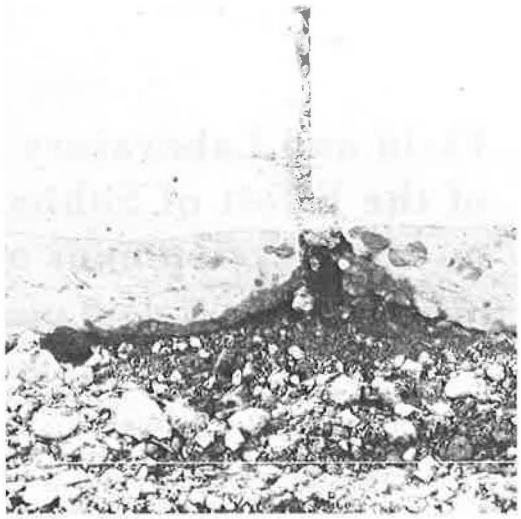

Figure 2. Transverse cross section of pavement in which severe D-cracking has developed. White line shows original bottom of pavement slab, lower half completely deteriorated.

FIELD OBSERVATIONS

The field observations were based on performance of more than 50 pavements located in Illinois, Iowa, Kansas, Minnesota, Missouri, Ohio, and Manitoba. Aside from inherent differences in durability of the coarse aggregates used, the findings underscored the importance of moisture availability and subbase drainage in the development of D-cracking. To cite an extreme comparison, bridge deck concrete that contained coarse aggregate from the same source as that used in the abutting pavement and in other pavements where D-cracking was extensively developed did not display similar evidence of aggregate failures. This may be explained by the fact that the underside of a bridge slab is not regularly exposed to free water or relative humidities of 100 percent, and thus the concrete is permitted to dry periodically and the aggregate to remain at a safe level of saturation.

Differences in subbase materials were found to affect the rate of development of D-cracking. In one section of Interstate pavement, D-cracking developed within 3 years where the concrete was placed on a granular subbase covered with a 1-mil

Figure 3. Vertical section of core taken through D-cracked pavement slab. Severe cracking in coarse aggregate particles extends into surrounding mortar.

thick polyethylene vapor barrier. In a nearby secondary pavement, in which the concrete was made with coarse aggregate from the same source but placed directly on a clay subgrade, only minor D-cracking appeared at a few transverse-longitudinal joint intersections after 7 years of service.

The importance of early moisture accumulation in base material was evident on a section of pavement built in 1950. After approximately 15 years of service, D-cracking had developed only in the southbound lane, which was placed directly on a rutted and water-filled clay subgrade immediately after a prolonged steady rainfall. In contrast, the northbound lane was placed at about the same time but on a relatively dry subgrade and showed no evidence of D-cracking.

The use of drainage facilities has been found, in some cases, to delay and possibly eliminate the development of D-cracking of the type that has been widely observed in pavements placed on granular subbases—both trenched in and carried through the shoulders. Schematic diagrams of the various pavement designs are shown in Figure 4. Figures 4a and 4b show widely used designs where there are no facilities provided to drain the subbase. D-cracking has developed with these designs at an early age in pavements containing susceptible aggregates. In these cases, moisture accumulated in the subbase more rapidly than it was able to drain away through the denser subgrade material; therefore, an environment was created where the lower levels of the pavement slab became critically saturated.

Three pavement designs with drainage facilities are shown in Figures 4c through 4e. In Figure 4c, longitudinal tile subdrains are contained in trenches backfilled with open-graded material to the bottom of the subbase. After less than 2 years, lateral drains extending from the longitudinal drains were found to be inoperative. Within 5 years, severe D-cracking had appeared at the pavement wearing surface.

Figure 4d shows a design where the trench was backfilled through the subbase. In this case, lateral drains were operating after 6 years and there was no evidence of D-cracking at the wearing surface where coarse aggregate was used from the same source as that in Figures 4b and 4c.

Figure 4e shows a later design where a positive drainage connector was installed between the trench and the pavement slab. After 3 years, lateral drains were functioning and there was no evidence of D-cracking at the wearing surface. However, it is too early to determine if this design is a durability improvement on the design in Figure 4d.

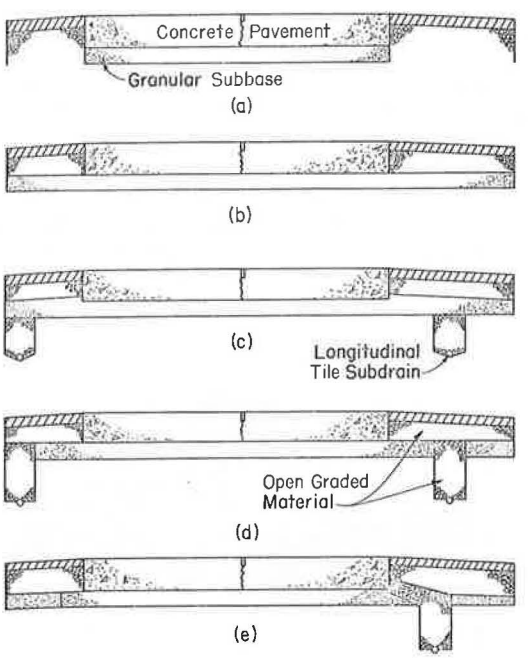

Figure 4. Pavement designs investigated in field studies.

CONTROLLED FIELD STUDIES

In view of these observations, a series of 4- by 5-ft by 6-in. thick concrete slabs containing coarse aggregates known to cause D-cracking were cast on subbases of various types in the outdoor test plot at the PCA laboratories. The primary purpose of these tests was to determine the effect of subbase type on moisture accumulation in the concrete slab. In view of the small scale on which these tests were to be made, it was considered impossible to install drainage facilities with the expectation of having them function in a manner similar to those used in highway construction.

Subbase Type and Construction

Four types of subbases were used in this study: granular, granular + 4-mil

polyethylene sheeting between the base and the slab, cement-treated, and clay. Details for these materials are given in Table 1. For the granular materials used for the cement-treated base, the cement content was 6.0 percent by weight and the water content was 7.8 percent by weight. The materials used for the clay subbase had the following characteristics: liquid limit, 29; plastic limit, 15; and plasticity index, 14. Subbases for each slab were carried 2 to 2½ ft beyond the test slab. The granular base material was used as it already existed in the test plot and was maintained at a nominal 6-in. thickness resting on existing clay loam soil. The clay subbase was placed directly on similar clay material underlying the clay loam, and was compacted in 8-in. layers and brought to the same grade as the granular material. The cement-treated base was compacted in 2 layers to a 6-in. thickness and covered with polyethylene until the test slabs were cast.

TABLE 1

GRADATION OF GRANULAR SUBBASE MATERIAL

Subbase	Sieve	Cumulative Percent Passing
Granular	1½ in.	100
	¾ in.	93.4
	No. 4	81.6
	No. 8	75.7
	No. 30	58.4
	No. 200	4.0
Cement-treated	1 in.	100
	¾ in.	92.5
	¼ in.	64.0
	No. 4	58.5
	No. 8	50.8
	No. 16	43.0
	No. 30	30.7
	No. 50	7.5
	No. 100	2.5
	No. 200	1.2

Concrete Slab Construction

Three coarse aggregates known to cause D-cracking were used in this study. These materials were obtained from limestone sources in Bethany Falls, Coralville, and Ervine Creek. Each of the aggregates was obtained from the stockpiles used for paving. Gradations and absorptions for these materials are given in Table 2. All slabs were cast in the fall of 1967. Before their use, the coarse aggregates were stockpiled and repeatedly hosed down and covered with burlap for 10 days. The sand used was obtained from Elgin, Illinois, whereas the cement was a laboratory blend of three commercial ASTM Type I cements produced in the Chicago area.

The mix design called for 6.8 bags of cement/cu yd and a water-cement ratio of 5 gal/bag. The air content was held at 6.0 ± 0.2 percent and the slump at 2 to 3 in. Following the initial floating, full-length, Y-shaped steel forms were vibrated into the slabs to a depth of 2 in. in order to procude "longitudinal" and "transverse" joints (Fig. 5). After the final finish, the slabs were covered with polyethylene. The following day the forms were stripped and vertical cracks were produced as extensions of the formed joints. For this work, numerous small, low-angle wedges were placed in the Y-shaped forms and driven downward until cracks could be observed on the vertical surfaces of the slabs. The forms were

TABLE 2

SUMMARY OF DATA FOR COARSE AGGREGATE

Coarse Aggregate Source	Gradation of Coarse Aggregate		Percent Absorption During 24 Hours
	Sieve	Cumulative Percent Passing	
Bethany Falls	1½ in.	100	1.74
	¾ in.	95	
	⅜ in.	37	
	No. 4	0	
Coralville	1½ in.	100	3.55
	¾ in.	77	
	⅜ in.	22	
	No. 4	0	
Ervine Creek	1½ in.	100	2.84
	¾ in.	60	
	⅜ in.	2	
	No. 4	0.8	

Figure 5. Form for casting test slabs and Y-shaped forms for making joints and cylinder mold used for concrete to be placed into cylindrical hole cast into slab.

removed, the joints were left unsealed, and granular material was compacted around the slabs, which were covered for curing with polyethylene for an additional 13 days.

Moisture Measurements

In order to monitor moisture movements in the test slabs, a method initially reported by the California Division of Highways was used (2). Cylindrical steel molds, machined to an outside diameter of 5.550 in., were positioned at centers 12 and 15 in. from the outside edges of the slabs (Fig. 5). These were removed from the slabs after approximately 6 hours. The concrete cylinders to be inserted into the holes thus formed were cast in steel molds machined to an inside diameter of 5.500 in. and equipped with centrally located 0.500-in. diameter steel rods, which were required to form a hole through which another rod could later be inserted to clamp the discs together. Concrete was taken from each batch for the appropriate slab and externally vibrated into the mold. After 1 day, the concrete cylinder was removed from the mold, placed in a plastic bag, and cured under polyethylene with the slab for 13 days. Companion reference cylinders were made each day of casting and cured in a similar manner.

Following the curing period, the cylinders were sectioned horizontally into six 1-in. thick discs whose sawed surfaces were finally lapped in water to permit intimate contact during the test exposure. A 0.500-in. diameter aluminum rod was then inserted into the centrally located hole and a 1-in. diameter rubber gasket and aluminum washer were fitted between the concrete and a steel nut to provide a tightly secured stack of discs. After insertion into the slab, the annular space in the hole was sealed with caulking material at the exposed surface. Weight measurements of each disc were made in the late fall and early spring to determine moisture changes just before and after the freezing season. After the 14-day cure, the companion cylinders were sliced and weighed. After moist-curing for an additional 2 to 3 months at 73 F, the slices were again weighed, and then oven-dried at 230 F to constant weight to determine the amount of evaporable water the concrete would hold under conditions of 100 percent relative humidity. Little or no weight change was recorded between the measurements at 14 days and at 3 months. Comparisons were then made between these measurements and those obtained from the test specimens.

Figure 6 summarizes the results of measurements according to subbase type after exposure to 2 freeze-thaw seasons. Each curve represents the average for the full depth of slabs made with 3 different coarse aggregates. It should be pointed out that the curves were derived from data obtained only during the months specifically indicated on the abscissa, and do not include the extreme effects of summer drying. An initial moisture increase of 3.7 to 6.3 percent was recorded after a 1-month, late fall exposure. The greatest average increase occurred in concrete placed on the clay subgrade. By April following the first freeze-thaw season, moisture contents had dropped 2 to 5 percentage points for concrete placed on the clay, cement-treated, and granular + vapor barrier bases but still remained above that immediately following an initial curing period. Moisture contents of concrete placed on the granular subbase dropped more than 4 percentage points to a level somewhat below that immediately following the initial curing period. Average moisture contents were nearly the same for the spring and fall measurements but then increased greatly during the fall season. The greatest increase was recorded for concrete placed on the cement-treated base. By December preceding the second freeze-thaw season, moisture contents were higher than the previous December only for concrete placed on the cement-treated and granular + vapor barrier subbases. During the second freeze-thaw season, moisture contents increased for concrete placed on the granular and clay subbases and remained constant or decreased for the other concretes. Following the most recent summer season, moisture contents were at higher levels than at any previous time.

Data for the bottom half of the concrete slabs are shown in Figure 7. It is seen that similar but less pronounced trends occur here compared with those for the full depth of the slab, except during the first month's exposure following the initial curing period. During this period, moisture increases were greater, as might be expected, because there was no direct exposure to atmospheric drying. Also, there was a slight change in the relative positions of the curves after 22 months' exposure. Comparison of the

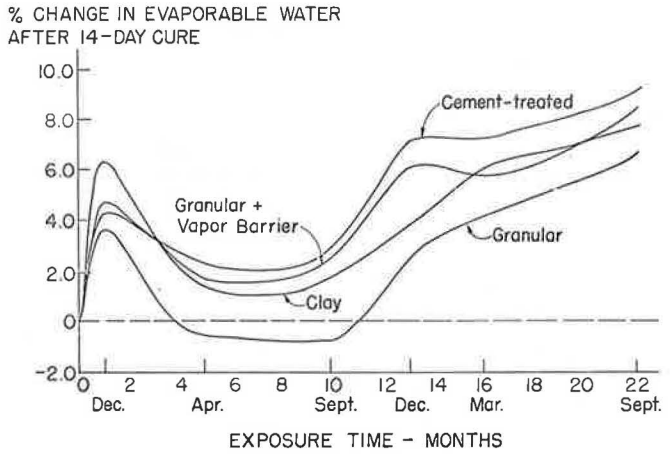

Figure 6. Moisture measurements for full depth of slabs on 4 subbases.

curves in Figures 6 and 7 shows that the bottom half of the slabs placed on the cement-treated and granular + vapor barrier subbases had smaller increases in evaporable water content compared with the full depth of these slabs.

Comparison of data for the full depth and bottom halves of the slabs placed on granular and clay subbases is shown in Figure 8. These curves indicate that greater moisture increases in the bottom half of the slabs during the first month's exposure following the 14-day curing period were more than maintained at later test ages. For example, differences between the full depth and bottom half of the slabs for the granular and clay subbases were 2.3 and 0.9 percentage points respectively after 1-month exposure, and 3.7 and 2.3 percentage points after an exposure of nearly 2 years. Similar results were obtained for concrete placed on the other two subbases.

As stated earlier, 3 different coarse aggregates known to cause D-cracking were used in this test series. Comparison of changes in moisture contents for the concretes containing these aggregates is shown in Figure 9. The curves suggest that the porosity of the coarse aggregate was a factor in the changes in moisture content, be-

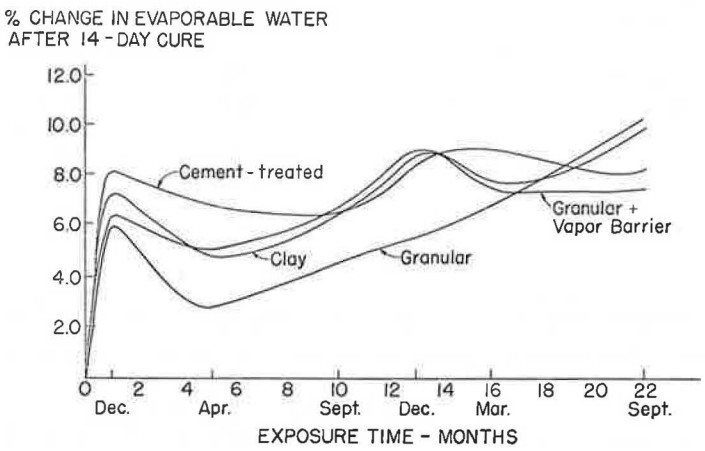

Figure 7. Moisture measurements for bottom half of slabs on 4 subbases.

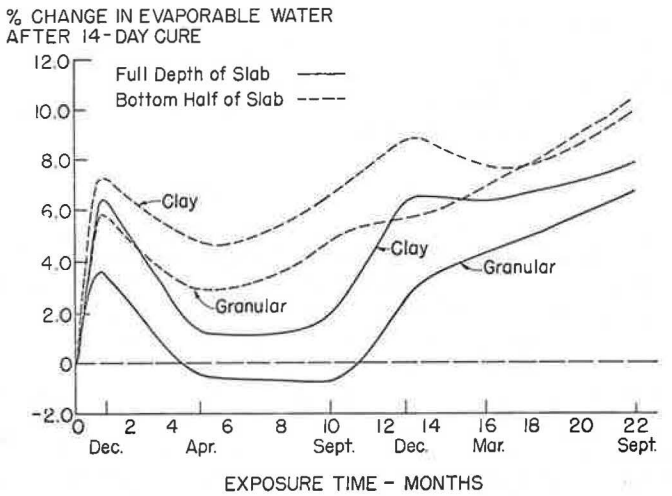

Figure 8. Moisture measurements for top and bottom halves of slabs placed on granular and clay subbases.

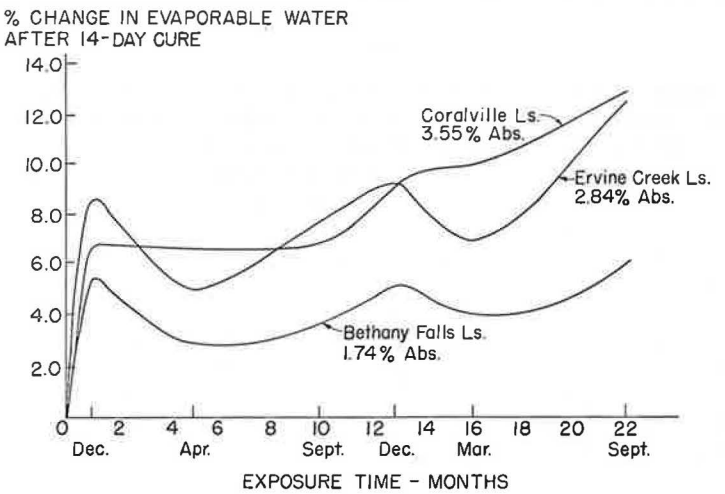

Figure 9. Moisture measurements for full depth of slabs made with 3 coarse aggregates.

cause the percent increase in evaporable water was lowest for concrete containing Bethany Falls limestone, which had the lowest vacuum absorption of 1.74 percent.

Petrographic Examination of Concrete

At the exposure age of 16 months, immediately following the second freeze-thaw season, 2 cores were taken from each of the concrete slabs, sectioned, and lapped longitudinally to study the extent of cracking in the coarse aggregate. Results showed that between 5 and 12 percent of the particles above those containing cracks in the unused aggregate were fractured in the concrete. The least amount of cracking was found in slabs placed on the clay and cement-treated bases and greatest amount in slabs

placed on the granular and granular + vapor barrier bases. In no instance was D-cracking apparent at the wearing surface. Apparently, moisture increases during the fall and winter seasons had been sufficient to critically saturate some of the coarse aggregate particles before freezing. However, the extent of cracking did not correlate with the percentage of moisture absorbed.

DISCUSSION OF FINDINGS

Several apparent precautions or limitations that must be considered in the procedure for measuring the moisture changes by this technique require that the results be interpreted with caution. First, the absolute values are probably not totally representative because the relative roughness of the interfaces would, on a submicroscopic scale, create relatively large voids between the much smaller capillaries in the cement paste and aggregate on both sides of the interface. The capillary flow between discs would thereby be disrupted. Later laboratory tests, in fact, substantiated this effect. Also, for concrete discs placed on the cement-treated and granular + vapor barrier subbases, there is no bonded contact between the concrete and underlying material. Therefore, free water may collect at this interface that would not otherwise be present, or it may evaporate more rapidly if leaks had developed in the seal in the annular space at the wearing surface. In addition, because a continuous shoulder composed of open-graded granular material was used between slabs (4 percent passing the No. 200 sieve), some evaporation may occur that would tend to minimize larger moisture differentials among slabs placed on the four types of subbases.

CONCLUSION

Although many precautions were taken in carrying out these tests, it is believed that the only conclusion that can be drawn from the moisture movement data is that a gradual increase in moisture content has occurred in these concrete slabs, regardless of the type of subbase. That these moisture increases were at one time sufficient to critically saturate certain coarse aggregate particles is indicated by the increase in the percentage fractured in the unused aggregate. Cracking of the type observed is similar to that which develops during the early stages of D-cracking in pavements.

Although field observations of pavements indicate that D-cracking can be delayed and possibly eliminated by the use of functional artificial drainage facilities, simulation and study of this factor have not yet been carried out under controlled laboratory conditions. However, studies of the D-cracking problem are continuing, and it is anticipated that work along these lines, together with tests to determine whether or not special drainage provisions would be beneficial with particular sources of coarse aggregate, will be conducted in the near future.

REFERENCES

1. Stark, David, and Klieger, Paul. Field and Laboratory Investigation of D-Cracking in Concrete Pavements.
2. Tremper, Bailey, and Spellman, D. L. Tests for Freeze-Thaw Durability of Concrete Aggregates. HRB Bull. 305, 1961, pp. 28-50.

Discussion

PHILIP D. CADY and ROGER E. CARRIER, Pennsylvania State University—In discussing the test method that he employed, the author voiced his concern regarding the discontinuity between the disc stack and the slab. If the annular area at the top of the slab is adequately sealed, the space between the discs and the slab should equilibrate at a relative humidity that will provide equal capillary filling in the discs and slab by the mechanism of capillary condensation. What appears to be of more concern to us

is the fact that the moisture exchange surfaces (the hole in the slab and the peripheral surfaces of the discs) are cast surfaces. We believe that a cast or finished concrete surface will have a vastly different pore system than the interior of the concrete. For one thing, the effect of the aggregate in moisture transport will be considerably altered because no aggregate is exposed at formed surfaces. Because of this, in experiments similar to those described by Stark, we used disc stacks sliced from concrete cores, where the disc stacks were tested in the core holes from which they were originally taken. During February 1968 through July 1969, our experiments were carried out in a pavement slab at a rest area on I-80 in central Pennsylvania. A rain gage was installed at the site and the disc installations and rain gage were monitored monthly. Four-in. diameter cores were taken from the 10-in. thick pavement slab and were subsequently cut into 6 discs approximately 1½ in. thick. A ⅜-in. diameter hole was drilled through the center of each disc. A large hole, 1 in. in diameter, was drilled through the top disc and a brass insert (topnut) was cemented in the hole using a weather-resistant epoxy glue. The top surface of this topnut was flush with the road surface. The six discs were bolted together with a ⅜-in. diameter brass bolt. O-shaped rubber gaskets were placed between the discs to cut off the annular space created by the core bit. The annular space at the top was sealed with an O-ring and caulking compound (Fig. 10).

Before insertion into the pavement, the discs were vacuum saturated (1½ hours of vacuum to 2 mm of Hg absolute with 24 hours of water submersion). Each disc was weighed (after damp drying the surface), and then oven-dried at 220 F to constant weight to establish the evaporable water content when saturated. They were then bolted together and inserted into the pavement. The two cores were placed 5 ft apart in 1 slab.

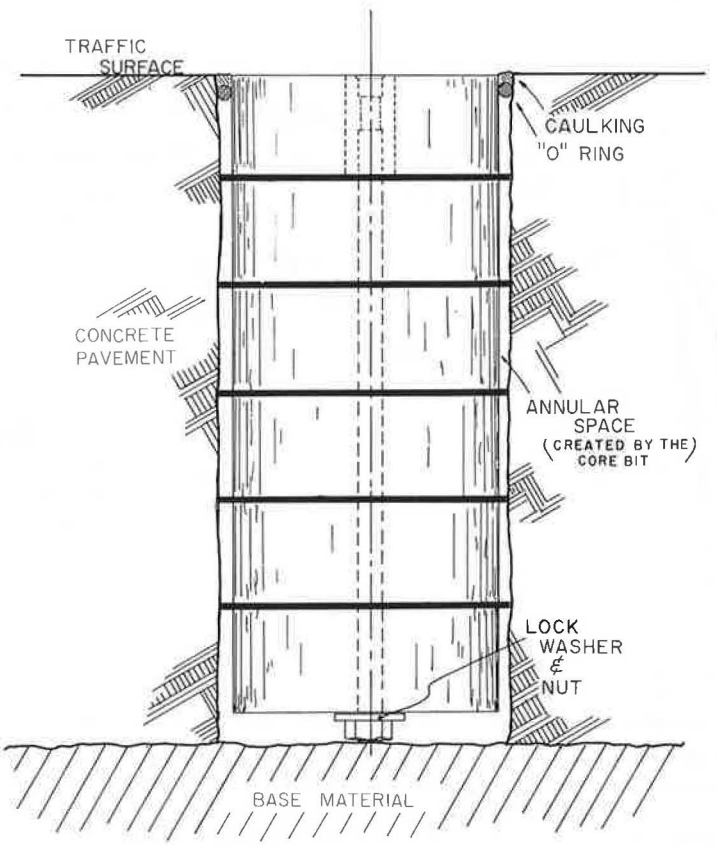

Figure 10. Test core placement in pavement slab.

The test slab was a part of a rest area on the eastbound lane of I-80, approximately 10 miles north of Clearfield, Pennsylvania. It is located on the southeastern slope of a hill, at an elevation of approximately 2,100 ft. The site lies over a thick-bedded, medium- to coarse-grained sandstone. The sandstone is well fractured and well drained. The 10-in. concrete slab is underlain by an 8-in. subbase (< 3-in. maximum crushed sandstone with a fairly uniform gradation) and 12 in. of granular material (essentially the same material). Because the test site lies on a sidehill location, little or no residual soil material lies between the granular material and the sandstone bedrock. In short, the pavement slab is well drained.

At the end of each month, the stacks of discs were removed. The surfaces were dried with a towel to a damp condition (SSD), and each disc was immediately weighed at the test site. After weighing, the stacks were reassembled, and inserted into the pavement. The O-ring was replaced and the annular space at the top was filled with caulking compound. To keep the top of the stack flush with the pavement, it was necessary to place a small layer of sand at the base of each core hole.

The nearby precipitation measuring stations could not offer valid data for rainfall at the test site because of the mountain topography that is atypical to this site. Thus, a rain gage with a 10-in. capacity was installed at the test site. It was placed in a cleared area to ensure proper exposure (lateral distance to nearest tall object was greater than twice that object's height, as recommended by rain gage manufacturer). Precipitation measurements were made on the last day of each month. Little evaporation occurred from the rain gage in the month period because of the small opening in the funnel in the top of the rain gage. In the winter months, the gage could not be read because the water had frozen and no thawing facilities were available at the test site.

The measured fluctuations in moisture content as well as the moisture distribution are shown in Figures 11 and 12. Results for December were not obtained because sev-

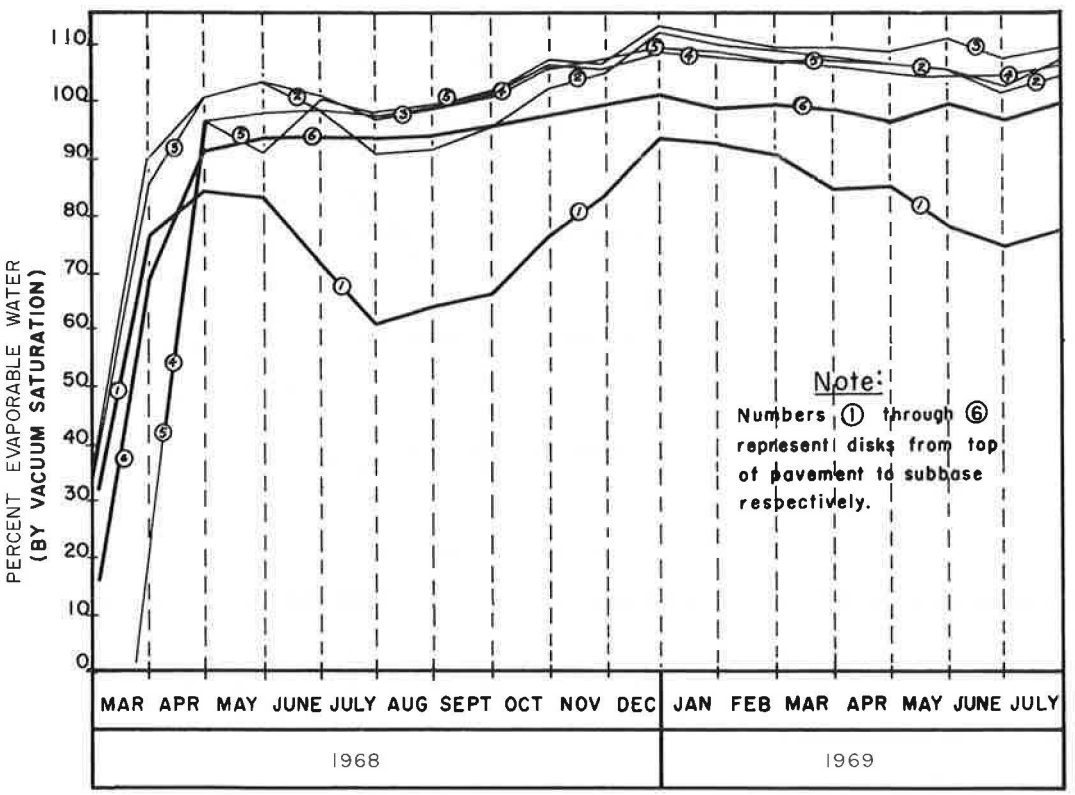

Figure 11. Moisture distribution in specimen A.

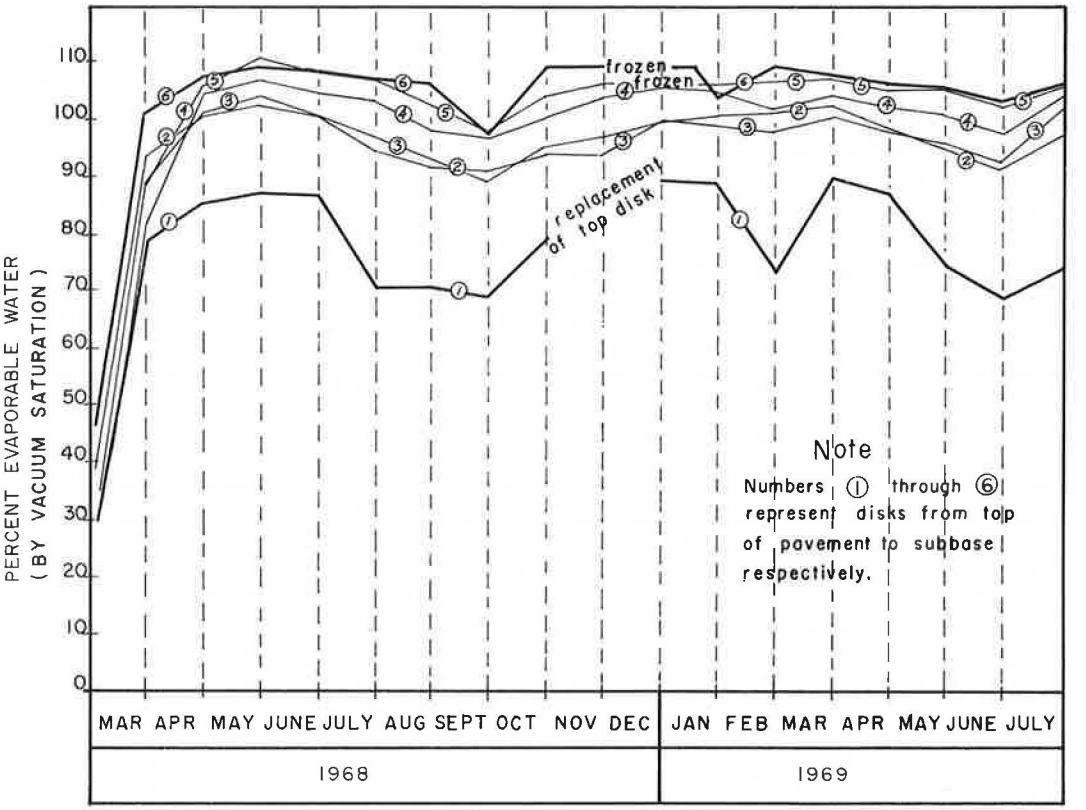

Figure 12. Moisture distribution in specimen B.

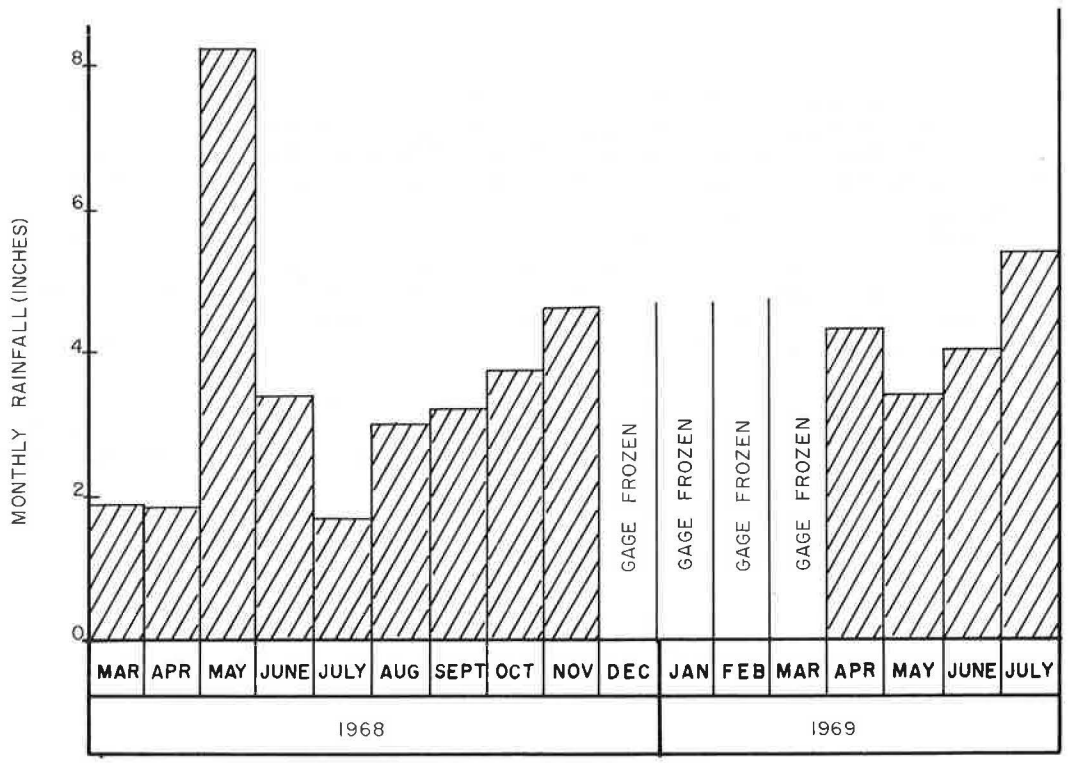

Figure 13. Monthly accumulation of rainfall.

eral of the discs became frozen fast in the slab. The rain gage data for the test period is shown in Figure 13.

As can be seen readily in Figures 11 and 12, the natural conditions allowed more water uptake than did the vacuum saturation; i.e., more than 100 percent of the evaporable water as here defined entered the discs when they were placed in the natural environment. Oven-dried specimens were placed in February 1968, and, for both cores, levels over 100 percent were reached by the end of April 1968. Those figures also show that, as might be expected, the lower discs always contained more moisture than the uppermost disc.

Traffic caused the top disc in specimen B to crack in November 1968 and it had to be replaced. It was discovered at the end of the test period that the epoxy bond in specimen A had failed sometime during the test, and it is felt that this caused the upper discs to become wetter than the lowest disc.

Note that in both cases, the upper 1½-in. thick disc seldom reached the critical 91.7 percent saturation level, the level above which freeze-thaw damage is probable. Note also that in both cases the lower discs seldom went below the 91.7 percent saturation level in the test period. There was evidence of slight flaking on the underside of some of the discs. Small flakes of mortar fell from these faces—especially from entrapped air pockets located on the undersides of these discs—to the top side of the next lower disc. These flakes appeared on the towel when the discs were toweled to the damp-dry condition. This occurred only in the winter months, but it never occurred on the top disc.

Note also from Figures 11 and 12 that the upper disc dries in the summer, as expected, but that the moisture content in the discs below that remains fairly constant. These discs are apparently not affected by seasonal changes in moisture.

We are currently carrying out similar experiments using disc stacks in concrete bridge decks. However, there is not enough data at this time to report on those installations.

DAVID C. STARK, Closure—In their discussion, Dr. Cady and Mr. Carrier point out another shortcoming in the reported procedure of using stacked discs to measure moisture contents; namely, the introduction of formed (cast) surfaces in the test material. They have apparently circumvented this problem by using concrete cores from which to construct the stacked discs.

The data in their discussion are interesting in that saturation levels greater than 100 percent (based on vacuum saturation) were reached within 1 year in the lower levels of the pavement slab. This finding supports our observations of D-cracking in pavements where deterioration in the form of fractures extending from coarse aggregate particles into the surrounding mortar have been noted in the lower levels of the slab after 1 year of exposure.

Although we are continuing to collect data of this sort in our outdoor test plot, we are presently exploring alternate methods of measuring moisture contents without having to cope with the type of precautions and uncertainties associated with this test procedure.

A Heat-Transfer Model for Evaluating Frost Action and Temperature-Related Effects in Multilayered Pavement Systems

BARRY J. DEMPSEY and MARSHALL R. THOMPSON, Department of Civil Engineering, University of Illinois

A heat-transfer model for evaluating frost action and temperature-related effects was developed for a multilayered pavement system. The heat-transfer model was derived from one-dimensional, forward-finite-difference, heat-transfer theory and has been programmed for computer solution. The model was designed to include many input parameters and it can be easily expanded to include newly developed parameters. The heat-transfer model can be used to evaluate the temperature regime of varied pavement systems in different geographical locations.

Meteorological parameters such as short-wave radiation, long-wave radiation, convection, and air temperature are the basic extrinsic factors used in the heat-transfer model. Intrinsic factors considered are the physical properties and thermal properties of the pavement materials that include unit weight, moisture content, material classification, thermal conductivity, heat capacity, and latent heat. The heat-transfer model was developed so that appropriate thermal properties of the pavement materials are used depending on whether the unfrozen, freezing, or frozen state exists.

Pavement temperatures generated by the heat-transfer model were compared with laboratory temperature data and temperature data from the AASHO Road Test, and the model was found to give valid results. Use of the heat-transfer model for evaluating frost action in a pavement system at a specified location was demonstrated for 30 years of past climatic record. It was shown that quantitative data necessary for evaluating frost action in pavement systems could be obtained. Also, a clearer understanding of the qualitative factors involved in frost action research was provided.

•THE DETERIMENTAL effects of frost action are a major problem and continue to be a significant cause of pavement deterioration leading to high maintenance costs. In many cases, the cost of annual repairs and maintenance is greater than the cost of preventive measures that might have been incorporated into the original pavement design and construction.

Completely acceptable techniques, procedures, and criteria have not been developed for adequately assessing freeze-thaw durability of pavement systems. Most laboratory durability testing procedures use arbitrary exposure conditions that are not representative of actual conditions in the field. Current durability criteria do not acknowledge the fact that climatic conditions (maximum and minimum air temperatures, sunshine, wind velocity, precipitation, etc.) vary with geographical location in many states. For example, the average winter temperature for northern Illinois is approximately 25 F, whereas that for southern Illinois is approximately 35 F.

Paper sponsored by Committee on Performance of Concrete—Physical Aspects and presented at the 49th Annual Meeting.

In recognition of the need for developing a reasonable and realistic procedure for evaluating frost action in pavement systems, research was undertaken with the following objectives:

1. Determine the factors that significantly influence frost action and temperature effects in pavement systems;
2. Develop a heat-transfer model that uses past climatic records for predicting frost action and temperature in multilayered pavement systems;
3. Validate the heat-transfer model by using laboratory and field data; and
4. Demonstrate how the heat-transfer model can be used to characterize frost action and temperature in typical pavement systems.

FACTORS INFLUENCING FROST ACTION IN PAVEMENT SYSTEMS

The number of published reports pertaining to frost action and its effects has grown to vast proportions. A review of literature by Johnson (1) made reference to more than 800 publications that dealt either entirely or partly with soil freezing and frost damage. Lovell and Herrin (2) have also summarized much of the earlier knowledge on soil freezing and related frost problems.

Because the nature of frost action is complex and involves many variables, no systematic approach can be taken to increase knowledge of the subject without first separating the major variables and determining their relative influence. In recognition of this, Johnson and Lovell (3) divided the factors that influence frost action into extrinsic and intrinsic categories.

The extrinsic factors shown in Figure 1 are those that are outside but that act directly on the soil. These factors specify the nature of the climate and modify the influence of climate on the depth and rate of freezing and thawing in pavement systems. Although both climate and load are major external factors (Fig. 1), Johnson and Lovell (3) indicated that climate is the most important factor to be considered.

The major intrinsic factors (state of the soil mass, the physical properties of the soil mass, the composition of the soil, and the thermal properties of the soil) influencing frost action are shown in Figure 2 and are those governed by the properties of the soil and its cover.

The influence of the various extrinsic and intrinsic factors shown in Figures 1 and 2 on frost action and temperature-related effects in pavement systems has been described

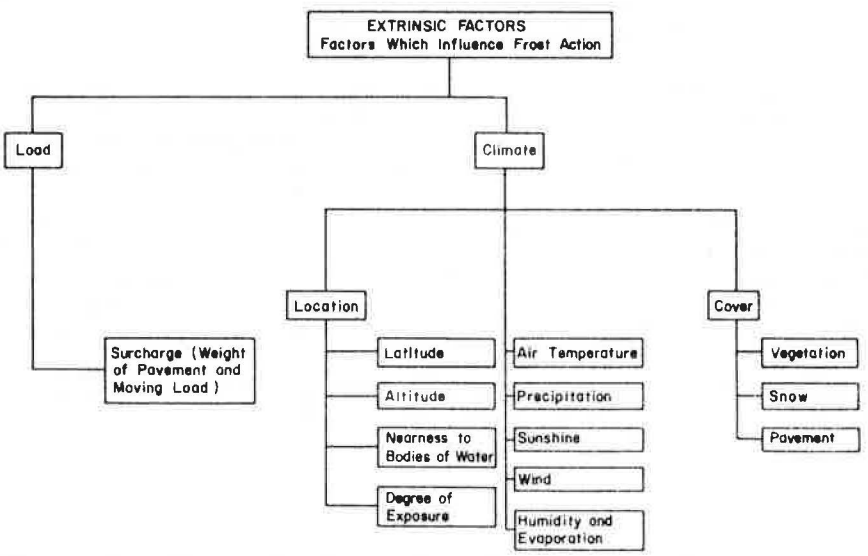

Figure 1. Extrinsic factors influencing frost action (3).

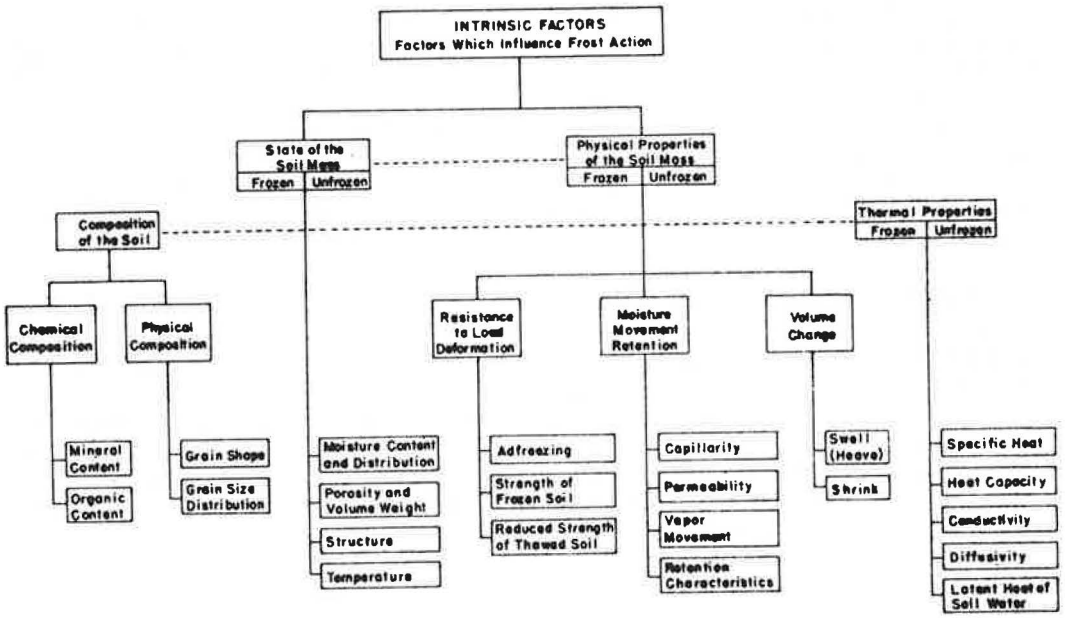

Figure 2. Intrinsic factors influencing frost action (3).

in detail by Dempsey (4) in other studies. Although there are differences of opinion concerning the relative importance of the various factors, it is generally agreed that the temperature variation of the earth at any location is caused by the climate of that area, and that the response of the soil and its cover to the climate is controlled by the thermal properties of the materials.

DEVELOPMENT OF A MODEL FOR EVALUATING FROST ACTION IN MULTILAYERED PAVEMENT SYSTEMS

A comprehensive literature review of the different methods for evaluating pavement temperatures indicated that a numerical method would be the most promising procedure for studying frost action in multilayered pavement systems with transient surface temperature conditions. The mathematics in the numerical method are simple, flexible, and well suited for programming on a digital computer. The method can be adapted to the complex heat-transfer conditions in multilayered pavements that occur as a result of changing thermal properties and changing climatic conditions.

Based on the initial success of several investigators (5, 6, 7), a one-dimensional, forward-finite-difference, heat-transfer model (hereafter referred to as heat-transfer model) was developed to evaluate frost action in multilayered pavement systems. In the heat-transfer model, the future temperature at a given nodal point is expressed as a function of time, its present temperature, and the present temperature of the adjacent nodal points. The finite-difference, heat-transfer equations were programmed on a digital computer so as to facilitate rapid solutions to large amounts of input data.

Studies by Aldrich (8), Straub, Dudden, and Moorhead (9), and Przybycien (10) have indicated that the assumption of one-dimensional heat transfer is applicable to the study of frost penetration below pavement surfaces. This is especially true in the case where the depth of frost penetration is small as compared to the pavement width.

In setting up the heat-transfer model, it was necessary to consider the basic mechanisms of heat transfer, which include conduction, convection, and radiation. The pavement system was divided into small vertical sections or nodes that had a cross-sectional area of 1 sq ft. The basic heat-transfer equations or a combination of these equations were used to relate the temperature of a specific node to the temperatures of

the surrounding nodes and to determine the temperature of the specific node after a given time increment. Because the temperature computed for a given node is the average for the entire volume, the temperature is specified at the center of the nodal volume.

The energy balance procedures used by Scott (11, 12, 13) and Berg (14) to relate pavement surface temperatures to meteorological parameters were incorporated into the heat-transfer model.

The factors associated with frost action are easily determined by analyzing the temperatures generated by the heat-transfer model for the various nodes in the pavement profile.

Finite-Difference Pavement System

Figure 3 shows a typical finite-difference pavement system used in the heat-transfer model for computing pavement temperatures. The pavement system consists of a column of nodes that have a cross-sectional area of 1 sq ft.

Nodes 2 through 37 are termed normal nodes. The nodal depth, ΔX, and the number of nodes are chosen so as to ensure mathematical stability and so that the interface between pavement layers will be located at a nodal center. Nodes 2 and 6 are also mixed nodes because the thermal properties of these nodes correspond in part to the thermal properties of the adjacent pavement layers.

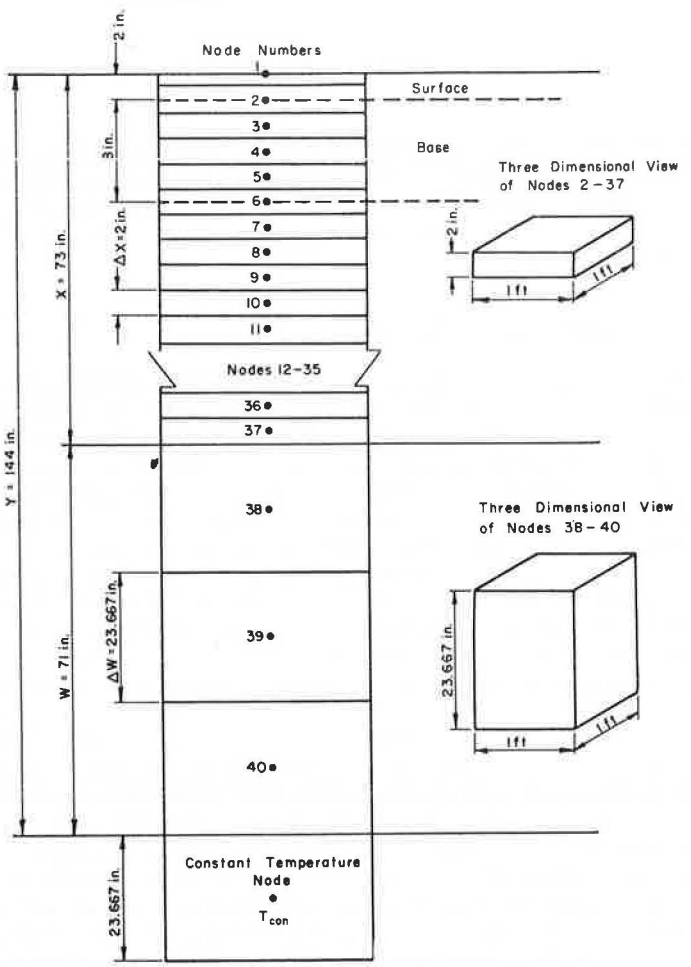

Figure 3. Typical finite-difference pavement system.

Node 1 consists of one-half of a normal node so that the nodal center will lie on the pavement surface. Node 1 at the pavement surface is the node at which the meteorological parameters are introduced and an energy balance is achieved.

Nodes 38, 39, and 40 are termination nodes and their purpose is to reduce computational time. The termination nodes replace the smaller nodes and reduce the total number of nodes in the finite-difference pavement system with only a small increase in the finite-difference error. Also, because the temperature variations decrease with increasing depth in the pavement, the increased depth of the bottom nodes, ΔW, will not cause a large increase in the computational error.

Flack (15) found that a finite-difference pavement system with a ratio of X/W of approximately one and three termination nodes would produce a finite difference error of less than 1 percent. He indicated that any termination strip configuration with more than three nodes would increase computational time without substantially reducing the error involved. Flack (15) further noted that the finite-difference error increased as the ratio X/W decreased and as the number of termination nodes decreased.

The total depth, Y, of the finite-difference pavement system is a variable input parameter in the heat-transfer model. It can be determined from a study of deep soil temperatures at a specified geographical location. For example, studies of soil temperatures in northern Illinois have indicated that the ground temperature remains essentially constant (51 F) at a depth of 29 ft, and that ground temperature fluctuations are relatively small (9 F or less) below a depth of 10 ft (16). It was concluded that a finite-difference pavement system with a depth of 144 in. (Fig. 3) could be used for Illinois because the ground temperature differences below this depth are quite small, and the additional cost in computer time required for a greater depth did not appear to be justified. At the bottom of the finite-difference pavement system, a constant temperature node was added to account for the outward flow of heat from the interior of the earth [noted by Thompson (17)]. The value of the constant temperature node is a variable input parameter in the heat-transfer model because it may vary with geographical location. A constant temperature of 51 F was considered to be a realistic temperature value for a soil depth of 144 in. in Illinois.

When using the finite-difference pavement system (Fig. 3), it is necessary to determine the initial nodal temperatures at the start of the investigation period. Carroll (18) has indicated that the initial pavement profile temperatures can be estimated provided that the heat-transfer model is initiated prior to the time accurate temperature predictions are to be made. He found that, although this approach would produce an initial error in the computed pavement temperatures, the error would decrease after a very short period of time as more climatic data were inserted into the heat-transfer model.

Page (19) has shown that the average date of the first killing frost is approximately October 13 in northern Illinois and approximately October 23 in southern Illinois. These findings indicate that a frost action study for Illinois should be started about October 1 so that the pavement profile temperatures generated by the heat-transfer model will converge by the time frost action begins to occur. Starting dates in other geographical locations can be based on the average date of the first killing frost.

Finite-Difference Equations

Convection and radiation play a dominant role in transferring heat between the pavement surface and air, whereas conduction plays a separate role in transferring heat within the pavement system. The procedure used to develop the finite-difference equations in the heat-transfer model was similar to that used by Straub et al. (5), Carroll et al. (7), and Schenck (20). (Symbols used in the following equations are defined in the Appendix.)

To illustrate the finite-difference solution, it is first necessary to transform the one-dimensional, Fourier, heat-transfer equation for transient heat flow into the finite-difference form. The general form of the one-dimensional, Fourier equation for conductive heat transfer is expressed as

$$\frac{\partial^2 T}{\partial X^2} = \frac{1}{\alpha} \frac{\partial T}{\partial \theta} \tag{1}$$

Kreith (21) has shown that the first and second derivatives in Eq. 1 can be replaced by the appropriate finite-difference terms and written as

$$\frac{T_{n-1} + T_{n+1} - 2T_n}{\Delta X^2} = \frac{1}{\alpha} \frac{T_n' - T_n}{\Delta \theta} \tag{2}$$

The thermal diffusivity, α, is equal to $K/C\gamma$. By arranging terms and substituting for α, Eq. 2 can be written for the heat balance on an arbitrary interior node as

$$\frac{K}{\Delta X}\left(T_{n-1} - T_n\right) + \frac{K}{\Delta X}\left(T_{n+1} - T_n\right) = \frac{\gamma C \Delta X}{\Delta \theta}\left(T_n' - T_n\right) \tag{3}$$

The terms $K/(\Delta X)\ (T_{n-1} - T_n)$ and $K/(\Delta X)\ (T_{n+1} - T_n)$ are the equations for the thermal conductivity of a nodal volume and the term $(\gamma C \Delta X)/(\Delta \theta)\ (T_n' - T_n)$ is the heat storage in a nodal volume during an incremental time period, $\Delta \theta$.

It is apparent that the one-dimensional, finite-difference solution consists of the basic heat-transfer equations and an energy balance on a specified node. The energy balance for an increment of time, $\Delta \theta$, can be expressed qualitatively as follows: Heat added to a nodal volume + heat given up by a nodal volume = heat stored in a nodal volume.

The finite-difference equations used in the development of the heat-transfer model have been described elsewhere by Dempsey (4).

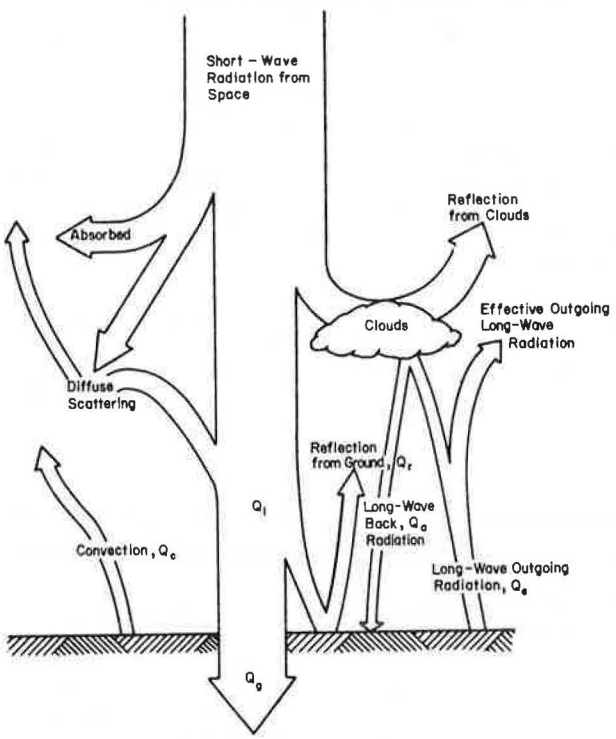

Figure 4. Heat transfer between pavement surface and air on a sunny day (8).

Meteorological Parameters

The most important parameters involved in the heat-transfer model are those related to the surface node. These are the meteorological parameters concerned with the net radiation heat transfer, Q_{rad}, and the convective heat transfer, Q_c, into or out of the pavement system (Fig. 4).

The finite-difference equation for the surface node is ideally suited for use with the meteorological energy balance approach proposed by Scott (11, 12, 13) and Berg (14). It is as follows:

$$Q_i - Q_r + Q_a - Q_e \pm Q_c \pm Q_h \pm Q_g = 0 \tag{4}$$

The degree of accuracy in predicting the pavement temperatures relies heavily on the choice of methods used to predict the radiation heat quantities and the convection heat quantity. Previous studies by Dempsey (4) have indicated that most equations are empirically determined from field and laboratory tests.

The importance of solar radiation in pavement temperature studies has been shown by Straub et al. (5) and Aldrich (8). From Eq. 4 the net amount of radiation, Q_{rad}, influencing heat transfer at the surface node is expressed as

$$Q_{rad} = Q_i - Q_r + Q_a - Q_e \tag{5}$$

The amount of incident short-wave radiation used in the energy balance at the surface node is determined by use of a regression equation developed by Baker and Haines (22) and expressed as

$$Q_i = R^* \left(A + B \frac{S}{100} \right) \tag{6}$$

The extraterrestrial radiation, R*, can be theoretically calculated for a given location from the solar declination, latitude, zenith angle, and solar constant.

In Figure 5, it is observed that the intensity of solar radiation varies parabolically from the time of sunrise to the time of sunset. Based on this observation, the amount of short-wave radiation received at the pavement surface during a finite-time increment, $\Delta\theta$, is calculated by assuming that the total daily extraterrestrial radiation varies in a parabolic manner from the time of sunrise to the time of sunset. The values for the total daily extraterrestrial radiation and the time of sunrise and sunset are easily used in the finite-difference program because they essentially do not change from year to year at any given geographical pavement location. Furthermore, the parabolic radiation distribution is readily programmed for a digital computer. The value of R* is obtained from the parabolic radiation distribution at any specified time during the day. The value of R* is taken as zero during nighttime.

Part of the incident short-wave radiation, Q_i, is lost as reflected short-wave radiation, Q_r. The amount of short-wave radiation reflected is a function of the incident short-wave radiation, Q_i, and the absorptivity, a, of the pavement surface as follows:

$$Q_r = (1-a)\, Q_i \tag{7}$$

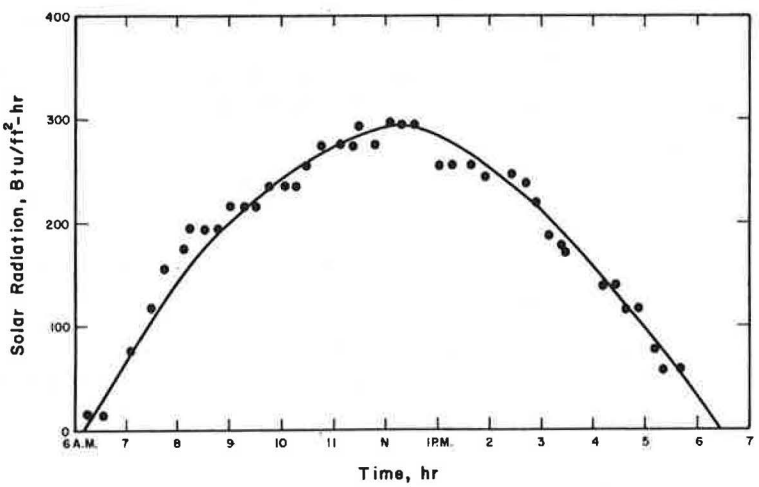

Figure 5. Variation in solar radiation intensity (5).

From Eqs. 6 and 7 the net amount of short-wave radiation that enters into the energy balance at the pavement surface, Q_s, is derived as follows:

$$Q_s = Q_i - Q_r \tag{8}$$

By substituting for Q_r in Eq. 8, the following equations are obtained:

$$Q_s = a\, Q_i \tag{9}$$

$$Q_s = a\, R^* \left(A + B \frac{S}{100} \right) \tag{10}$$

Essentially, Eq. 10 considers the influence of cloud cover, reflection from the clouds, diffuse scattering, absorption by the atmosphere, and reflection by the pavement surface on the extraterrestrial radiation.

An analysis of variance test on the constants A and B in Eq. 10 for more than 10 years of record at 6 radiation stations in the Midwest (Indianapolis, Indiana; Lansing, Michigan; Madison, Wisconsin; Columbia, Missouri; Ames, Iowa; and Lemont, Illinois) showed that there was no significant difference, $\alpha = 0.05$, between the various stations or within a given station. Therefore, it appears that average values of the constants A and B can be used for determining quantities of short-wave radiation in many geographical locations. The average value of A is 0.202 and the average value of B is 0.539 for the six midwestern states analyzed. The percentage of possible daily sunshine, S, can be obtained at any first-order Environment Sciences Services Administration (ESSA) Weather Bureau Station (formerly designated as United States Weather Bureau Station).

The long-wave radiation entering into the energy balance at the pavement surface consists of the long-wave radiation emitted by the pavement, Q_e, and the long-wave back radiation emitted by the atmosphere, Q_a. The long-wave radiation emitted from a unit area of pavement surface with no correction for cloud cover, Q_x, is expressed by the following theoretical equation:

$$Q_x = \sigma \epsilon T_{1R}^4 \tag{11}$$

The emissivity, ϵ, varies according to the type of pavement surface, wave length, and average temperature of the pavement. The Stefan-Boltzmann constant, σ, has a value of 0.172×10^{-8} Btu/hr-ft^2-R^4.

Q_z, the long-wave back radiation affecting the energy balance at the pavement surface with no correction for cloud effects, is determined by an empirical formula developed by Geiger (23) as follows:

$$Q_z = \sigma T_{airR}^4 \{ G - J(10^{-\rho p}) \} \tag{12}$$

In considering the work of a number of investigators, Geiger (23) assigned the following values to the constants in Eq. 12: G = 0.77, J = 0.28, and $\rho = 0.074$. The vapor pressure, p, in Eq. 12 can generally be considered to vary between 1 and 10 mm of mercury for climate near the ground surface (23).

Using the suggestion of Scott (13) that the net long-wave radiation entering into the energy balance at the pavement surface be corrected for cloud cover in a manner similar to that for short-wave radiation, an approach recommended by Geiger (23) was used as follows:

$$Q_e = Q_x \left(1 - N \frac{\overline{W}}{100} \right) \tag{13}$$

$$Q_a = Q_z \left(1 - N \frac{\overline{W}}{100}\right) \tag{14}$$

In Eqs. 13 and 14, N is a cloud-base factor whose value ranges between approximately 0.90 and 0.80 for cloud heights between approximately 1,000 ft and 6,000 ft respectively (23). These cloud heights are realistic for many geographical locations during the winter months. The percentage of cloud cover, $\overline{W}$, is equal to 0 percent for cloudless days and 100 percent for completely overcast days. $\overline{W}$ can be computed from the percentage of possible daily sunshine as follows:

$$\overline{W} = 100 - S \tag{15}$$

If average daily climatic input data are used in the heat-transfer model, it is necessary to assume that the percentage of cloud cover during the daytime carries into the nighttime also.

The rate of heat transfer by convection, Q_c, between the pavement surface and air is computed by the following method for a unit surface area:

$$Q_c = H \left(T_{air} - T_1\right) \tag{16}$$

The convection coefficient, H, is difficult to estimate because of the many variables involved. Previous studies by Dempsey (4) have shown that most investigations involving the convection coefficient have not been concerned with pavement surfaces. Most of the formulas apply to vertical walls and roofs of buildings.

An empirical formula developed by Vehrencamp (24) appears to be the most applicable to a pavement surface. He developed an empirical formula for determining the convection coefficient by using data obtained from a very large, very smooth, hard-packed, dry lake bed. The formula for determining the convection coefficient is as follows:

$$H = 122.93 \left\{0.00144\ V_m^{0.3} U^{0.7} + 0.00097 \left(V_1 - V_{air}\right)^{0.3}\right\} \tag{17}$$

The surface temperature, V_1, and the air temperature, V_{air}, are both in degrees centigrade. V_m is the average of the air temperature and pavement surface temperature in Kelvin degrees temperature, and it is calculated as follows:

$$V_m = 273.0 + \frac{V_1 + V_{air}}{2} \tag{18}$$

The wind velocity, U, in Eq. 17 is the average daily wind velocity in m/sec. Since the original equation developed by Vehrencamp (24) gave the convection coefficient in terms of g-cal/min-cm^2-C, Eq. 17 contains a factor of 122.93 to give the convection coefficient, H, in the more familiar units of Btu/hr-ft^2-F.

Equation 17 takes into consideration both the forced convection resulting from wind turbulence and free convection resulting from the buoyancy effect of air.

The maximum value of the convection coefficient is controlled to some extent by the mathematical stability requirement established by the forward-finite-difference approach.

When using the radiation heat-transfer equations and convection heat-transfer equation at the pavement surface node, it is necessary to develop a method for determining the air temperature after each time increment, $\Delta\theta$. Generally most ESSA Weather Bureau Stations record only the maximum and minimum daily air temperatures without regard to the times at which these temperatures occur. To provide a continuous daily

temperature record for the heat-transfer model, it was necessary to determine the times at which the maximum and minimum temperatures occurred and interpolate between these times for intermediate temperatures.

Straub et al. (5) have shown that during a typical winter day the temperature varies according to a sine wave so that generally the minimum daily air temperature occurs early in the morning and the maximum daily air temperature occurs in the early afternoon. An analysis of the hourly pavement surface temperatures at the AASHO Road Test at Ottawa, Illinois, during 3 winter seasons showed that the average time of occurrence of the minimum daily temperature was about 4:00 a. m., and the average time of occurrence of the maximum daily temperature was about 1:00 p. m. for both portland cement concrete and asphalt concrete pavements. These findings indicated that the approximate times at which the minimum and maximum air temperatures occurred in Illinois during winter could be estimated as 4:00 a. m. and 1:00 p. m. respectively.

Scott (11, 12, 13) and Berg (14) indicated that heat transfer caused by transpiration, condensation, evaporation, and sublimation, Q_h, could be neglected without greatly affecting the energy balance at the pavement surface. Both Scott (11) and Berg (14) expressed formulas for determining the heat transfer by several of these methods; however, they found the results obtained by the formulas to be highly variable and totally unpredictable.

In the development of the heat-transfer model, the effects of transpiration, condensation, evaporation, and sublimation were neglected because of the uncertainty of their values at this time. Large error was not expected to be created in the energy balance at the pavement surface by assuming Q_h as zero. Transpiration can be neglected in pavement studies because this is related to vegetation growth. The heat flux resulting from condensation is lost when the condensate evaporates. Heat transfer by evaporation should be minimal if rainwater quickly drains off the pavement surface. Because snow removal from most pavements takes place shortly after the snow has fallen, heat flux caused by sublimation can also be disregarded.

Heat fluxes resulting from precipitation and moisture infiltration into the pavement system were not included in the energy balance because there is no accurate procedure to calculate these heat quantities at the present time. Furthermore, the extent of surface moisture infiltration is questionable and highly dependent on the type and condition of the pavement surface (25, 26, 27). For ideal pavement conditions, the heat flux caused by infiltration can be considered negligible.

Thermal Properties of Pavement Materials

The most important intrinsic factors considered in frost action are the thermal properties of the pavement materials, which include thermal conductivity, heat capacity, and latent heat of fusion. The heat-transfer model recognizes three different sets of thermal properties depending on whether the pavement material is in an unfrozen, freezing, or frozen condition.

The procedures for determining the thermal properties of the pavement materials have been described in detail by Dempsey (4). The thermal properties of the surface materials were determined from general tables of physical properties or from scientific research. The methods developed by Kersten (28) were found to be suitable for determining the thermal properties of the base, subbase, and subgrade soils.

The heat capacity of a pavement material during freezing is determined from the latent heat of fusion of the moisture in the material. When the moisture in the pavement freezes, the portion that is about to change phase remains at a constant temperature, the freezing temperature, until the latent heat of fusion is released. The time lag caused by this process retards the rate of frost penetration. The latent heat effect is incorporated into the finite-difference equations by using an approach described by Schenck (20), which makes use of a freezing zone. The freezing zone is a small, hypothetical temperature range over which freezing takes place. Because only moisture effects are considered in this range, the freezing heat capacity, C_f, in the freezing zone is a function of the moisture content, dry density, and the small freezing temperature range.

In the development of the heat-transfer model, the freezing zone was set at a 2 F temperature interval between variable input temperatures of 30 F and 32 F. The freezing heat capacity, C_f is calculated as follows:

$$C_f = \frac{144w\,\gamma_d}{200\gamma} \tag{19}$$

Equation 19 is divided by the total unit weight, γ, in order to be properly used in the finite-difference equations.

A comparison of the freezing heat capacity and unfrozen and frozen heat capacities for a granular base material with about 9 percent moisture is shown in Figure 6. It should be noted that even for a small moisture content the freezing heat capacity of the moisture is far greater than the unfrozen and frozen heat capacities of the material itself.

VALIDATION OF THE HEAT-TRANSFER MODEL

The validity of the heat-transfer model was established by using temperature data from laboratory studies and the AASHO Road Test at Ottawa, Illinois.

Initial temperature studies were made in the laboratory because these facilities provided for close control over the factors influencing heat transfer in soils. In the laboratory study, it was possible to determine whether the thermal properties of soils computed by the proposed methods were satisfactory and to study the influence any variations in the thermal properties would have on pavement temperatures predicted by the heat-transfer model.

A typical comparison between the measured temperature and theoretical temperature at the 6-in. depth in a composite laboratory specimen during a 13-day time period is shown in Figure 7. The general laboratory results revealed that the heat-transfer model accurately predicts soil temperatures.

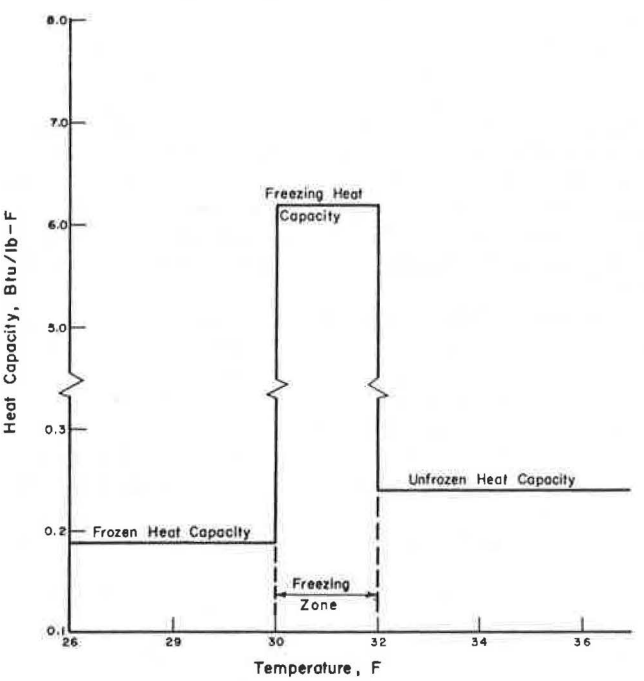

Figure 6. Effect of temperature on the heat capacity of a granular base material.

The theoretical temperatures computed by the heat-transfer model were compared with measured temperatures for a test pavement at the AASHO Road Test to see if the model would work properly under field conditions. A more detailed discussion of the AASHO test pavement, thermal properties, and climatic data can be found in a previous report by Dempsey (4).

For the purpose of evaluating the heat-transfer model, a winter period from October 1, 1959, through March 31, 1960, was analyzed. Because pavement temperatures near the surface vary within a given day as well as from day to day, comparisons between the theoretical temperatures and measured temperatures were made at 6:00 a. m. and 3:00 p. m.

Figure 8 shows a graphical comparison between the

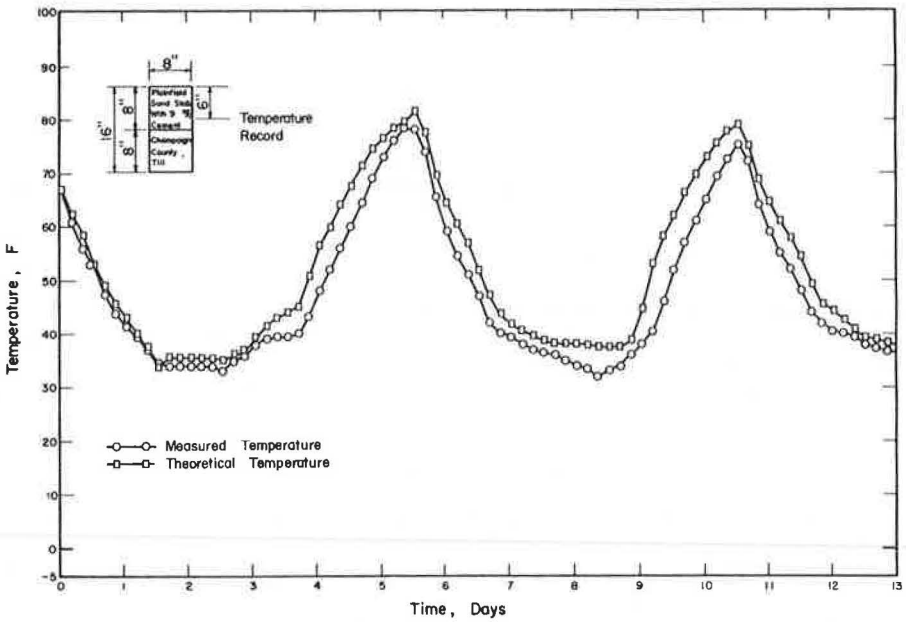

Figure 7. Comparison of measured and theoretical temperatures at 6-in. depth in a composite laboratory specimen.

measured temperature and theoretical temperature at the bottom of a 6-in. pavement surface at 6:00 a. m. The average difference between the measured temperature and theoretical temperature is 0.97 F.

A typical grpahical comparison between the measured temperature and theoretical temperature at 3:00 p. m. is shown in Figure 9. The average difference between the measured temperature and theoretical temperature is 0.73 at the 3-in. depth.

The validity of the heat-transfer model was further checked by comparing the number of freeze-thaw cycles predicted by the model with the number of freeze-thaw cycles in the actual pavement at the AASHO Road Test. Freezing in the pavement was considered to occur whenever the pavement temperature reached 30 F or less and remained at that temperature for more than 2 hours. Similarly, thawing was considered to occur whenever the pavement temperature exceeded 30 F and remained above that temperature for more than 2 hours.

At a depth of 3 in. in the pavement, 41 freeze-thaw cycles were determined from the theoretical temperatures as compared to 38 freeze-thaw cycles determined by analyzing the measured hourly temperatures. At the 6-in. depth, 15 theoretical freeze-thaw cycles were observed as compared to 17 freeze-thaw cycles determined from the measured temperatures for the test pavement at the AASHO Road Test.

Temperature comparisons for the subgrade would have been desirable, but measured data from the AASHO Road Test were not available. However, good agreement between the theoretical and measured temperatures at depths of 3 and 6 in. indicated that good temperature comparisons at greater depths would also exist if the thermal properties of the paving materials are carefully determined.

The excellent comparisons between the theoretical temperatures and measured temperatures and the good agreement between the number of freeze-thaw cycles at various depths indicate that the heat-transfer model is valid for predicting temperatures for use in frost action studies in multilayered pavement systems.

APPLICATIONS OF HEAT-TRANSFER MODEL

Engineering construction is greatly influenced by climate. The type of structure, its design, and its operation and maintenance are all affected by meteorological

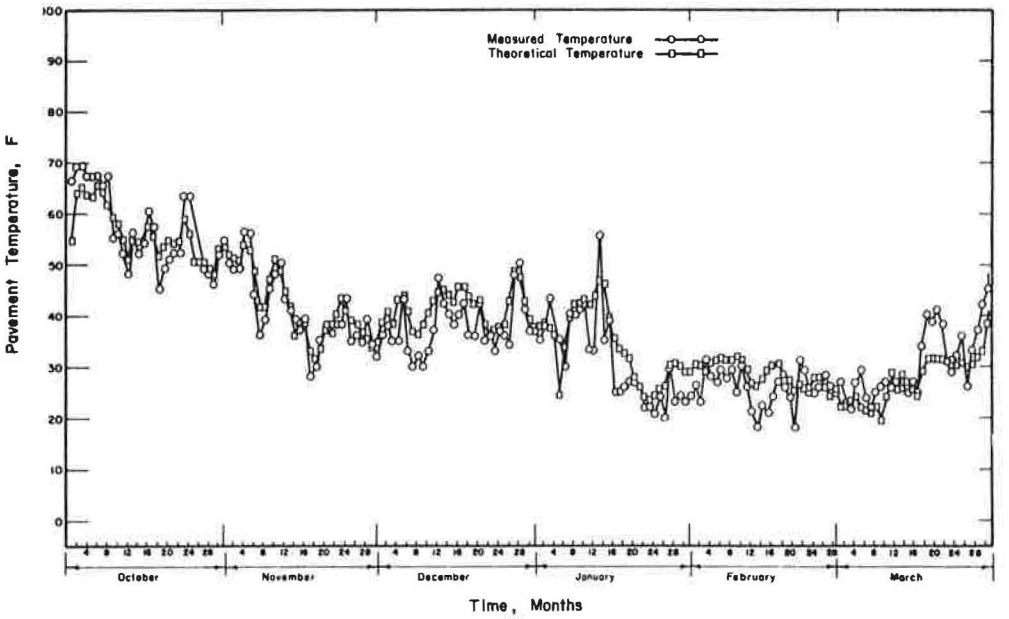

Figure 8. Comparison of measured and theoretical temperatures at the 6-in. depth of a 6-in. asphalt concrete pavement at 6:00 a. m. (AASHO Road Test, 1959 to 1960).

conditions. To evaluate properly the effect of these conditions on a structure, it is necessary to have a knowledge of the climate in which the structure is to be built and

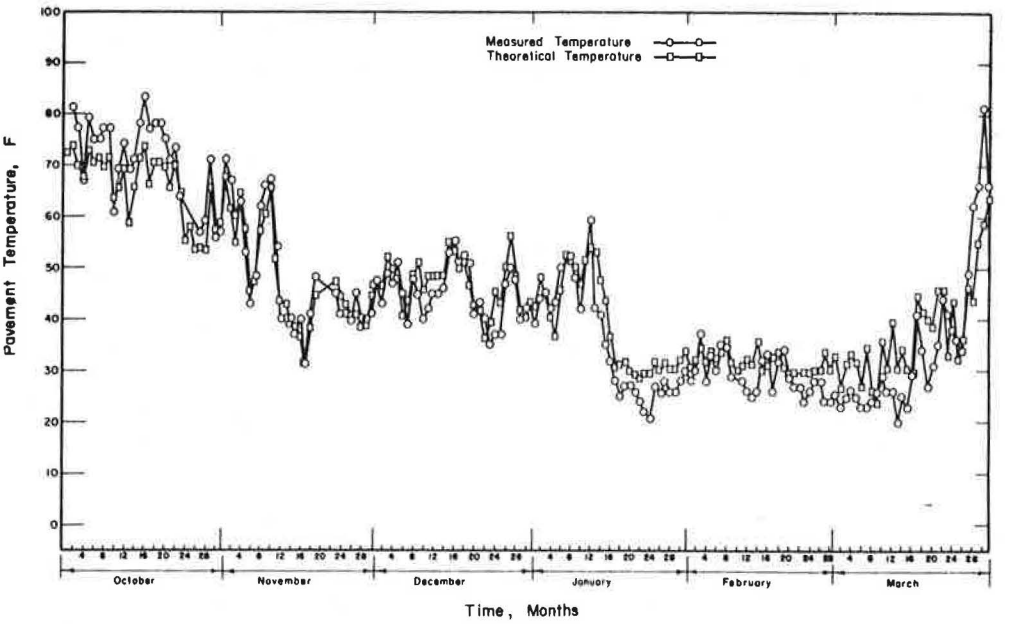

Figure 9. Comparison of measured and theoretical temperatures at the 3-in. depth of a 6-in. asphalt concrete pavement at 3:00 p. m. (AASHO Road Test).

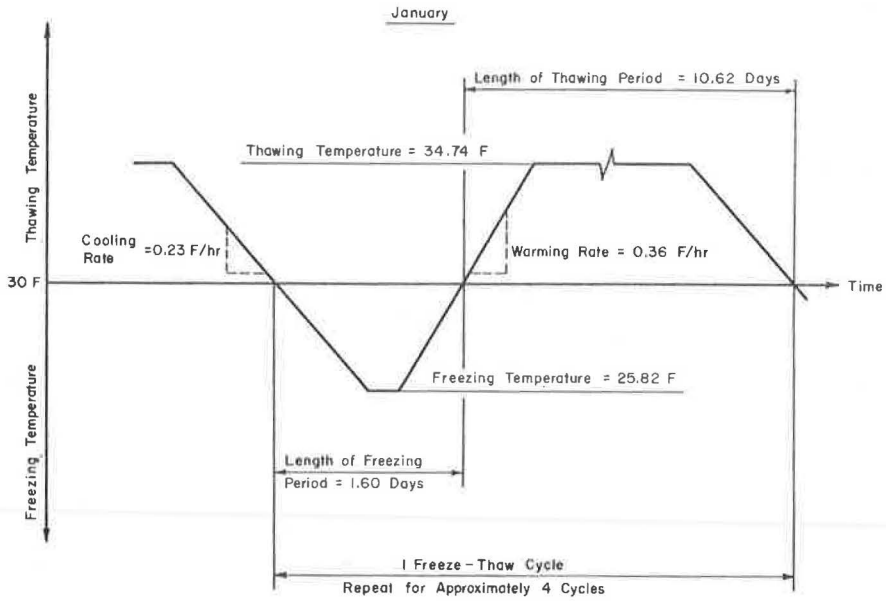

Figure 10. Characteristic frost action cycle.

to understand how the relevant meteorological parameters should be considered in its design, construction, and operation.

The heat-transfer model has application to an extensive range of engineering systems that are influenced by environmental factors. Thompson and Dempsey (29) have used the heat-transfer model to study frost action in pavement systems at various geographical locations in Illinois. Figure 10 shows a characteristic frost action cycle for central Illinois in January that was obtained by use of the model.

The heat-transfer model has numerous other applications in the areas of cold weather construction, asphalt pavement design, placement of underground utilities, and design of insulated pavements.

DISCUSSION OF HEAT-TRANSFER MODEL

Only a basic outline of the heat-transfer model has been presented in this report. A more detailed presentation of the development, validation, and utilization of the heat-transfer model can be found in previous work by Dempsey (4).

The heat-transfer model, which was developed by using basic heat-transfer theory, provides a means for accurately predicting temperatures in multilayered pavement systems. The model is very flexible and ideally suited for the study of frost action in pavements. It can be used for any pavement system, meteorological conditions, and geographical location.

The accuracy of the temperatures predicted by use of the heat-transfer model depends mainly on the quality of the input data and not the numerical methods of solution. The surface energy balance provided the most comprehensive procedure for incorporating the meteorological parameters into the heat-transfer model. It was important that the boundary conditions at the pavement surface be properly programmed because they are the major factors contributing to heat transfer in the pavement.

Close agreement between the measured and theoretical temperatures for laboratory and field data indicated that the assumptions, idealizations, and approximations made during the development of the heat-transfer model were sufficiently correct. Average differences between the measured temperatures and theoretical temperatures for depths of 3 and 6 in. in a test pavement at the AASHO Road Test were approximately 1 F.

In developing the heat-transfer model, the thermal properties were considered to be unaffected by changing moisture conditions. This assumption is reasonably correct because the thermal conductivity term and heat capacity term as used in the heat-transfer equation counteract each other to some extent. In general, the use of thermal properties that are not corrected for changing moisture conditions is considered to furnish good temperature results provided the moisture changes are small.

It is apparent that improvement in the accuracy of the pavement temperatures predicted by the heat-transfer model will result if a comprehensive procedure for analyzing moisture changes in the pavement system is developed. The procedure would have to consider the influence of such factors as the groundwater table, percolating rainwater, snowmelt, and unsaturated flow in the soil.

It was found during this investigation that usable field data for checking the heat-transfer model were difficult to find. The main reason for this problem was the fact that most available pavement temperature measurements in the field were made at sporadic time intervals. In this study, field temperature measurements recorded hourly during each day were found to be best suited for checking the temperatures predicted by use of the heat-transfer model. Hourly temperature records are especially desirable when making temperature comparisons near the pavement surface because these temperatures can vary considerably within a single day. It was evident from this study that field temperature measurements that have been made at regular time intervals and that have been well documented are needed for future model checks. It is also necessary to record other climatic conditions such as maximum and minimum air temperatures, wind velocity, amount of daily sunshine, rainfall, snowfall, and relative humidity. The condition of the pavement surface (snow cover, precipitation, cleanness, etc.) should also be recorded.

The heat-transfer model can be used to provide more complete records of pavement temperatures than field studies. The model provides a fast, efficient, and economical method for determining temperatures for frost action studies in pavement systems based on many years of climatic record. Complete frost action analyses, which would include characterizing frost action at five or six critical depths in a pavement system for a period of 10 years, would require approximately 60 min of IBM 360/75 computer time. It is apparent that the cost would be considerably less than that required for even a short-duration frost action study of 1 or 2 years in the field. Instrumentation and labor costs would exceed the cost of using the modeling procedure after a very short time. Therefore, it is apparent that the heat-transfer model provides an economical as well as accurate procedure for predicting frost action in pavement systems.

SUMMARY AND CONCLUSIONS

Summary

An investigation was conducted to develop a satisfactory and realistic procedure for evaluating frost action in multilayered pavement systems. Climatic data were the major input information required. An extensive literature review was conducted to determine the extrinsic and intrinsic factors that were important to the development of a heat-transfer theory for a pavement system. The various methods for predicting pavement temperatures and frost depth were investigated. Based on available information, a heat-transfer model was developed to evaluate frost action in multilayered pavement systems. The theoretical temperatures predicted by use of the heat-transfer model were checked with laboratory data and with field data, and the heat-transfer model was determined to be valid.

While checking the heat-transfer model, it was found that the quality of the input data would exert considerable control on the accuracy of the predicted temperatures. It was apparent that the heat-transfer model was adaptable to the climatic data for any geographical location and for any pavement system.

The application of the heat-transfer model to the study of frost action in a typical pavement system was demonstrated. It was determined that the heat-transfer model was satisfactory for characterizing frost action and temperature-related effects in multilayered pavement systems.

Conclusions

From the results of this investigation, the following conclusions were made:

1. The one-dimensional, forward-finite-difference, heat-transfer model provides a valid means for predicting pavement temperatures for evaluating frost action.
2. The approach developed furnishes frost penetration data as well as detailed predictions of temperatures throughout the pavement profile based on past climatic record.
3. The heat energy balance method used to relate meteorological conditions to the pavement surface temperature provides a comprehensive approach to temperature predictions in pavements.
4. Long-wave and short-wave radiation are important heat energy sources affecting pavement temperatures.
5. The heat-transfer model can be used to predict quickly and economically temperatures and depths of frost penetration in pavements over long periods of time.
6. The heat-transfer model displays potential uses for many types of environmental research.

ACKNOWLEDGMENTS

This study was conducted as a part of the Illinois Cooperative Highway Research Program Project IHR 401, Durability Testing of Stabilized Materials, by the staff of the Department of Civil Engineering, in the Engineering Experiment Station, University of Illinois, under joint sponsorship of the Illinois Division of Highways and the U. S. Department of Transportation, Federal Highway Administration, Bureau of Public Roads.

The opinions, findings, and conclusions expressed in this report are those of the authors and not necessarily those of the state of Illinois, Division of Highways, or the Bureau of Public Roads.

REFERENCES

1. Johnson, A. W. Frost Action in Roads and Airfields. HRB Spec. Rept. 1, 1952.
2. Lovell, C. W., Jr., and Herrin, M. Review of Certain Properties and Problems of Frozen Ground, Including Permafrost. SIPRE Rept. 9, Eng. Exp. Sta., Purdue Univ.; Snow, Ice, and Permafrost Research Establishment, Corps of Engineers, U. S. Army, Wilmette, Ill., 1953.
3. Johnson, A. W., and Lovell, C. W., Jr. Frost Action Research Needs. HRB Bull. 71, 1953.
4. Dempsey, B. J. A Heat-Transfer Model for Evaluating Frost Action and Temperature Related Effects in Multilayered Pavement Systems. Thesis, Dept. of Civil Engineering, Univ. of Illinois, Urbana, 1969.
5. Straub, A. L., Schenck, H. N., Jr., and Przybycien, F. E. Bituminous Pavement Temperature Related to Climate. Highway Research Record 256, 1968, pp. 53-77.
6. Corlew, V. S., and Dickson, P. F. Methods for Calculating Temperature Profiles of Hot-Mix Asphalt Concrete as Related to the Construction of Asphalt Pavements. AAPT, Atlanta, Ga., 1968, pp. 20-23.
7. Carroll, C., Schenck, H., Jr., and Williams, W. Digital Simulation of Heat Flow in Soils. Jour. Soil Mech. and Found. Div., Proc. ASCE, Vol. 92, No. SM4, 1966, pp. 31-49.
8. Aldrich, H. P., Jr. Frost Penetration Below Highway and Airfield Pavements. HRB Bull. 135, 1956, pp. 124-149.
9. Straub, A. L., Dudden, P. F., and Moorhead, F. T. Frost Penetration and Moisture Changes Related to Highway Pavement Shoulder Color. Highway Research Record 276, 1969, pp. 39-49.
10. Przybycien, F. E. Bituminous Pavement Temperature Related to Climate. Thesis, Dept. of Civil Engineering, Clarkson College of Technology, Potsdam, N. Y., 1967.

11. Scott, R. F. Heat Transfer at the Air-Ground Interface With Special Reference to Freezing and Thawing Problems Below Airfield Pavements. Thesis, M. I. T., Cambridge, 1955.
12. Scott, R. F. Estimation of the Heat-Transfer Coefficient Between Air and the Ground Surface. Trans., Amer. Geophysical Union, Washington, D. C., Vol. 38, No. 1, 1957.
13. Scott, R. F. Heat Exchange at the Ground Surface. U. S. Army Material Command, Cold Regions Research and Engineering Laboratory, Hanover, N. H., 1964.
14. Berg, R. L. Energy Balance on a Paved Surface. U. S. Army Terrestrial Sciences Center, Hanover, N. H., 1968.
15. Flack, W. J. The Application of Termination Strips to One-Dimensional Transient-Heat-Flow Solutions. Thesis, Dept. of Civil Engineering, Clarkson College of Technology, Potsdam, N. Y., 1965.
16. Fifteen Year Climatologic Summary. Argonne National Laboratories, Lemont, Ill., 1968.
17. Thompson, W. A. Soil Temperature at Winnepeg, Manitoba. Scientific Agriculture, Vol. 15, No. 4, 1934.
18. Carroll, C. S. A One-Dimensional Digital Simulation of Frost Penetration. Thesis, Dept. of Civil Engineering, Clarkson College of Technology, Potsdam, N. Y., 1965.
19. Page, J. L. Climate of Illinois. Agri. Exp. Sta., Urbana, Ill., Bull. 532, 1949.
20. Schenck, H., Jr. Fortran Methods in Heat Flow. The Ronald Press Company, New York, 1963.
21. Kreith, F. Principles of Heat Transfer. Internat. Textbook Co., Scranton, Penn., 1966, pp. 240-244.
22. Baker, D. G., and Haines, D. A. Solar Radiation and Sunshine Duration Relationships in the North-Central Region and Alaska. Exp. Sta., Univ. of Minnesota, Technical Bull. 262, 1969.
23. Geiger, R. The Climate Near the Ground. Harvard Univ. Press, Cambridge, Mass., 1959.
24. Vehrencamp, J. E. Experimental Investigation of Heat Transfer at an Air-Earth Interface. Trans., Amer. Geophysical Union, Vol. 34, No. 1, 1953, pp. 22-29.
25. Kersten, M. S. Progress Report of Special Project on Structural Design of Non-rigid Pavements—Survey of Subgrade Moisture Conditions. HRB Proc., Vol. 24, 1944, pp. 497-515.
26. Kubler, G. Influence of Meteorologic Factors on Frost Damage in Roads. Highway Research Record No. 33, 1963, pp. 217-255.
27. Moulton, L. K., and Dubbe, E. C. A Study of the Relationship Between Air Temperatures and Depth of Frost Penetration as Related to Pavement Performance of West Virginia's Highways. State Road Commission Rept. No. 7, Eng. Exp. Sta., West Virginia Univ., Morgantown, 1968.
28. Kersten, M. S. Thermal Properties of Soils. Bull. 28, Eng. Exp. Sta., Univ. of Minnesota, Minneapolis, 1949.
29. Thompson, M. R., and Dempsey, B. J. Quantitative Characterization of Cyclic Freezing and Thawing in Stabilized Pavement Materials. Highway Research Record 304, 1970, pp. 38-44.

Appendix A

DEFINITION OF SYMBOLS

The symbols used in the finite-difference equations are defined in the following:

A = radiation equation constant;

a = absorptivity of radiation by a surface;
B = radiation equation constant;
C = general mass heat capacity designation, Btu/lb-F;
C_f = mass heat capacity of a freezing material, Btu/lb-F;
G = Geiger constant;
H = convection coefficient, Btu/hr-ft^2-F;
J = Geiger constant;
K = general thermal conductivity designation, Btu/hr-ft-F;
N = cloud-base factor;
p = vapor pressure, mm;
Q_a = heat flux resulting from long-wave radiation emitted by the atmosphere, Btu/ft^2-hr;
Q_c = heat flux resulting from convective heat transfer, Btu/ft^2-hr;
Q_e = heat flux resulting from long-wave radiation emitted by the pavement surface, Btu/ft^2-hr;
Q_g = heat flux conducted into pavement, Btu/ft^2-hr;
Q_h = heat flux resulting from transpiration, condensation, evaporation, and sublimation, Btu/ft^2-hr;
Q_i = heat flux resulting from incident short-wave radiation, Btu/ft^2-hr;
Q_r = heat flux resulting from reflected short-wave radiation, Btu/ft^2-hr;
Q_{rad} = net radiation flux influencing heat transfer at a surface, Btu/ft^2-hr;
Q_s = net short-wave radiation entering into the energy balance at the pavement surface, Btu/ft^2-hr;
Q_x = long-wave radiation emitted from a surface without cloud cover correction, Btu/ft^2-hr;
Q_z = long-wave back radiation not corrected for cloud cover, Btu/ft^2-hr;
R^* = extraterrestrial radiation, Btu/ft^2-day;
S = percentage of possible daily sunshine, percent;
T_1 = temperature of surface node, F;
T_{1R} = Rankine temperature of surface node, F;
T_{air} = air temperature, F;
T_{airR} = Rankine temperature of air, F;
T_{con} = temperature of constant temperature node, F;
T_n = nodal temperature, F;
T_n' = nodal temperature after a time step, F;
U = wind velocity, m/sec;
V_1 = surface temperature, C^e;
V_{air} = air temperature, C^e;
V_m = average of air temperature and surface temperature in Kelvin temperature, C^e;
W = total depth of termination nodes, ft, in.;
$\overline{W}$ = percentage of cloud cover at night, percent;
ΔW = depth of a termination node, ft, in.;
w = water content based on dry weight, percent;
X = total depth of normal nodes, ft, in.;
ΔX = depth of a normal node, ft, in.;
Y = total depth of finite-difference pavement system, ft, in.;
α = thermal diffusivity, $K/C\gamma$, ft^2/hr;
γ = total unit weight, pcf;
γ_d = dry unit weight, pcf;
ϵ = emissivity of radiation by a surface;
$\Delta\theta$ = time step, hr;
ρ = Geiger constant; and
σ = Stefan-Boltzmann constant, 0.172×10^{-8}, Btu/hr-ft^2-R^4.